

Fall 2016

The Investigation of The Electrical Control of Hemimicelles and Admicelles on Gold for Analyte Preconcentration

Dheyaa Hussein Al-Karawi

Western Kentucky University, dheyaa.al-karawi345@topper.wku.edu

Follow this and additional works at: <http://digitalcommons.wku.edu/theses>



Part of the [Analytical Chemistry Commons](#), [Inorganic Chemistry Commons](#), and the [Other Chemistry Commons](#)

Recommended Citation

Al-Karawi, Dheyaa Hussein, "The Investigation of The Electrical Control of Hemimicelles and Admicelles on Gold for Analyte Preconcentration" (2016). *Masters Theses & Specialist Projects*. Paper 1732.
<http://digitalcommons.wku.edu/theses/1732>

This Thesis is brought to you for free and open access by TopSCHOLAR®. It has been accepted for inclusion in Masters Theses & Specialist Projects by an authorized administrator of TopSCHOLAR®. For more information, please contact topscholar@wku.edu.

THE INVESTIGATION OF THE ELECTRICAL CONTROL OF HEMIMICELLES
AND ADMICELLES ON GOLD FOR ANALYTE PRECONCENTRATION

A Thesis
Presented to
The Faculty of the Department of Chemistry
Western Kentucky University
Bowling Green, Kentucky


In Partial Fulfillment
Of the Requirements for the Degree
Master of Science

By
Dheyaa Hussein Ibrahim Al-Karawi

December 2016

THE INVESTIGATION OF THE ELECTRICAL CONTROL OF HEMIMICELLES
AND ADMICELLES ON GOLD FOR ANALYTE PRECONCENTRATION

Date Recommended 11-3-2016




Dr. Eric Conte, Director of Thesis



Dr. Stuart Burris



Dr. Darwin Dahl



Dean, Graduate Studies and Research

11/14/16

Date

Acknowledgments

I'm taking the advantage of this opportunity to express my gratitude to the people who support me throughout my research journey. Without their support, my thesis would never have been accomplished.

Primarily, I would like to thank my research advisor Dr. Eric Conte for his guidance, support, and trust. His door was always open for me whenever I ran into trouble or had a question about my research. He consistently allowed this work to be my own work, but he advised me in the right direction whenever I needed it. He also provided me the opportunity to work on another project after I finished with my first one trying to expand my research vision and my scientific knowledge by going further in the field of analytical chemistry. I appreciate him, his precious time, his motivations, and encouragements to move forward in this research.

I also will never forget the unlimited guidance, support, and time that Dr. Stuart Burris, department chair and my research committee member, provided me regarding the electrochemistry part of my research. He was very supportive and helpful when I had an issue or question regarding my research trying to figure out what other choices are potentially applicable for me.

I would also like to acknowledge Dr. Darwin Dahl for being a member of my research committee, and employing his valuable time to make that happen. I am gratefully indebted to him for accepting to be a member of my research committee.

I cannot really express how I'm grateful to Dr. John Andersland for all the support and guidance regarding the plating part of my research and his suggestions for coating

woven Monel and nickel mesh with gold. He also provided me a Scanning Electron Microscopy "SEM" training course. I also appreciate him for helping me to take high-quality SEM images of my specimens.

Additionally, I would like to express my heartfelt gratitude to some people who had a fascinating input in my research. I would like to thank Dr. Jacek Lipkowski (professor at the department of chemistry, University of Guelph, Guelph, Ontario, Canada N1G 2W) for the guidance and suggestions regarding the electrochemistry part of my research. I also would like to thank Mrs. Alicia Pesterfield for her chemical supply help and cooperation with me as a researcher to keep our research laboratory running and moving forward in the research process. In addition, I would like to thank Mrs. Haley Smith for her cooperation and facilitating my paperwork in the chemistry department office. I also would like to express my appreciation to my research mate Christopher Fullington for all the support and the assistance he provided throughout my research. Also, I would like to thank him for being a good listener when I needed him.

Moreover, I would like to express my gratitude to the Higher Committee for Education Development in Iraq (HCED) for the financial support.

Last but not least, I would like to thank all my friends for their support. I also must express my very profound gratitude to my family for providing me with unfailing support and continuous encouragement throughout my years of study and through the process of researching and writing this thesis. I would like to express my profound gratitude for my parents, who passed away, for all the love, encouragements, and support throughout my life journey. I hope they hear me; I always pray to God that they may enter into his paradise. I also would like to extend my deepest appreciation and respect to

the woman who has stood with me and given her time to me. She is my wife, Baraa Al-Maamouri. I would certainly say that none of my accomplishments would have come to life without her.

Thank you

TABLE OF CONTENTS

1. Introduction	1
1.1 Overview	1
1.2 Background: the application of hemimicelle and admicelle in the analytical chemistry	3
2. Experimental part	16
2.1 Standard solutions	17
2.2 Major instrumentations and materials were used	17
2.3 Capacitance measurements for monitoring the formation of DS monolayer on positively charged gold substrates	19
2.4 The column procedure involving three steps	20
2.4.1 The control experiment	20
2.4.2 The electric field blank experiment	21
2.4.3 Preconcentration experiment	21
2.5 Anthracene control experiment	23
2.6 9-anthracenecarboxylic acid control experiment	24
2.7 Micro-Lab techniques for gold deposition on Monel alloy	25
2.7.1 Cleaning procedure	25
2.7.2 Activation Solutions and plating procedure	26
2.8 The process of Nickel coated with Gold	27

3. Results and discussion	29
3.1 Capacitance measurements for monitoring the formation of DS monolayer on positively charged gold substrates	29
3.2 The column procedure	31
3.2.1 The control experiment	32
3.2.2 The electric field blank experiment	33
3.2.3 Preconcentration experiment	36
3.3 Anthracene control experiment	39
3.4 9-Anthracenecarboxylic acid control experiment	43
3.5 The process of Monel coated with Gold: scanning electron microscope SEM images	45
3.5.1 Eventual failure of Monel column material following multiple electrochemical experiments.....	50
3.6 The process of nickel coated with gold: scanning electron microscope SEM images	54
3.6.1 The evaluation of nickel gold-coated column.....	59
4. Conclusion	62
5. Bibliography	64

TABLE OF FIGURES

Figure 1. Micelle, hemimicelle, and admicelle structures in an aqueous solvent [9].	4
Figure 2. Schematic of micellar solubilization.	5
Figure 3. Surfactant molecules at low concentrations (monomers) and high concentration (micelles).	6
Figure 4. Stages of solid phase extraction (SPE).	8
Figure 5. The capacitance measurement with different SDS concentrations after 80 cycles.	15
Figure 6. The chemical structure of 2-naphthol.	16
Figure 7. The chemical structure of Sodium dodecyl sulfate (SDS).	17
Figure 8. Nickel gold-coated column.	18
Figure 9. Nickel gold-coated pieces (3 x 4 cm ²).	19
Figure 10. Capacitance measurements at three different stages: Stage I: 1 mM Na ₂ SO ₄ ; Stage II: 4 mM SDS in 1 mM Na ₂ SO ₄ ; Stage III: 2ppm 2-naphthol in 1 mM Na ₂ SO ₄ .	29
Figure 11. Schematic representation of the capacitance measurements that shown in Figure 10.	30
Figure 12. The differences in peak areas for three samples: 2 ppm 2-naphthol, 2-naphthol (premixing sample), 2-naphthol after 4-5 min of mixing.	33
Figure 13. 2-naphthol destruction test: 1: 2 ppm of 2-naphthol, 2: 2-naphthol with no potential applied, 3: 2-naphthol at 0.6 V for 45 minutes.	35
Figure 14. 2-naphthol destruction test: 1: 2 ppm 2-naphthol, 2: 2-naphthol with no potential applied, 3: 2-naphthol at 0.8 V for 45 minutes.	35

Figure 15. The effect of using different electrolytes on 2-naphthol concentration with an applied potential of 0.6 V vs. Ag/AgCl.	36
Figure 16. The preconcentration experiment of 2ppm 2-naphthol and 4 mM SDS at 0.6 V vs. Ag/AgCl; where A: 2 ppm of 2-naphthol, B: Control test, C: Preconcentration at an applied potential of 0.6 V, D: Releasing stage when the cell was turned off, and E: Rinsing with 10 mL of 70% methanol.	37
Figure 17. The preconcentration experiment of 2 ppm 2-naphthol and 6 mM SDS at 0.6 V vs. Ag/AgCl; where A: 2 ppm of 2-naphthol, B: Control test, C: Preconcentration at an applied potential of 0.6 V, D: Releasing stage when the cell was turned off, and E: Rinsing with 10 mL of 70% methanol.	39
Figure 18. Anthracene adsorption onto gold substrates during the two-hour test.	40
Figure 19. Mass balance measurements for anthracene adsorption onto gold substrates.	41
Figure 20. Anthracene adsorption onto nickel substrates during the two-hour test.	42
Figure 21. Mass balance measurements for anthracene adsorption onto nickel substrates.	43
Figure 22. 9-anthracenecarboxylic acid adsorption onto gold substrates during the two-hour test.	44
Figure 23. Mass balance measurements for 9-anthracenecarboxylic acid adsorption onto gold substrates.	45
Figure 24. Inactivated Monel and overexposure to the activation solution.	47
Figure 25. Monel alloy emersion time in activation solution.	48
Figure 26. Top: 3 seconds activation; Bottom: Original Monel alloy mesh.	48
Figure 27. Monel gold-coated (left); Un-coated Monel alloy (right).	49
Figure 28. Elemental analysis of areas (1) and (2) in Figure 27.	49

Figure 29. SEM image of the corrosion field of the Monel alloy.....	51
Figure 30. Plating fracture and exposed Monel alloy.	52
Figure 31. SEM image marked with integration data of the elemental analysis of Monel column material.	52
Figure 32. Elemental analysis of areas (1, 2, 3, and 4) in Figure 31.	53
Figure 33. The visible corrosion of the column material after disassembly and before analysis with SEM.	53
Figure 34. SEM image for nickel gold-coated and uncoated nickel mesh.	54
Figure 35. A magnified SEM image for the uncoated nickel mesh at 5kX using SEI mode.....	55
Figure 36. Elemental analysis of area (1) in Figure 35.....	55
Figure 37. SEM image for nickel coated with gold at 10kX using SEI mode.....	57
Figure 38. Elemental analysis of areas (1) and (2) in Figure 37.....	57
Figure 39. SEM image for nickel coated with gold at 5kX using BEI mode.	58
Figure 40. SEM image for nickel coated with gold at 20kX using SEI mode.....	58
Figure 41. SEM image after 18 months for a used nickel gold-coated column at 1kX using SEI mode.	60
Figure 42. A magnified SEM image at 5kX for the area marked in Figure 41 using SEI mode.....	60
Figure 43. Elemental analysis of areas (1, 2, and 3) in Figure 42.	61

THE INVESTIGATION OF THE ELECTRICAL CONTROL OF HEMIMICELLES AND ADMICELLES ON GOLD FOR ANALYTE PRECONCENTRATION

Dheyaa Al-Karawi

December 2016

67 Pages

Directed by: Dr. Eric Conte, Dr. Stuart Burris, and Dr. Darwin Dahl

Department of Chemistry

Western Kentucky University

Hemimicelles and admicelles are well-investigated wonders in modern science; they are surfactant monolayers and surface adsorbed micelles, respectively. Capacitance measurements for monitoring the formation of dodecyl sulfate (DS) surfactant monolayer on positively charged gold substrates (planar gold) and the adsorbance of 2-naphthol onto DS surfactant monolayer were performed. The investigation of the electrical control of DS at various concentrations (4, 6, 16, and 32 mM) below and above the critical micelle concentration ($CMC = 8 \text{ mM}$) on gold surfaces for analyte preconcentration, prior to chromatographic analysis, is presented. Charged ionic surfactants, such as DS, drawn to a surface of opposite charge (porous nickel substrates coated with gold) serve as a stationary phase to trap organic analytes. It is believed that these DS assemblies gain stability through surfactant chain-chain interactions. The attachment and the removal of the surfactant are controlled using an electric field. Due to the fact that the surfactant-analyte association is released by electrical control, organic solvents, which are used in conventional solid phase extraction, are not required, making this procedure environmentally friendly. Electrical Impedance Spectroscopy was used to investigate the formation of the DS layer and the preconcentration of 2-naphthol in the presence of an applied electric field. High performance liquid chromatography was used to determine 2-naphthol concentrations. Anthracene and 9-anthracenecarboxylic acid were substituted as additional test molecules as well. Presented are the results of the preconcentration of 2-

naphthol, anthracene and 9-anthracenecarboxylic acid using the DS layer with various concentrations of sodium dodecyl sulfate on a gold electrode surface.

Keywords: Hemimicelles, Admicelles, Micelles, Preconcentration, Organic analytes.

1. Introduction

1.1 Overview

Solid-phase extraction (SPE) at present is the most popular sample preparation method. This technique has been applied to a wide range of compound classes and has undergone considerable development in recent years, with many improvements in formation, automation, and the introduction of new phases. Its acceptance in routine analysis as an alternative to liquid-liquid extraction is increasing in different areas—mainly environmental monitoring—where several official methods for analysis of organic compounds in drinking water and wastewater use SPE as the sample preparative method [1].

Supramolecular assemblies have been largely used in analytical extraction and concentration schemes. Techniques, for example, include micellar-enhanced ultrafiltration, cloud point extraction, coacervation, surfactant-assisted transport of solutes across liquid membranes, and reverse micellar extractions [2-6]. These have been extensively developed in the recent years, and their basic features and practical applications are also established. Micellar-enhanced ultrafiltration (MEUF) is a method for the elimination of numerous organic and inorganic pollutants from an aqueous phase. This process uses the great efficacy of reverse osmosis and the high flux of ultrafiltration. The main principle is to increase the size of pollutant molecules by forming a complex with surfactants [2]. Cloud point extraction is the separation and preconcentration of target analytes using non-ionic and anionic surfactants [3]. Coacervation is the process of forming liquid rich in polymer phase in balance with an alternative liquid phase [4]. The liquid membrane process includes the transport of a solute from an aqueous phase

through an immiscible organic phase to a new aqueous phase [5]. Reverse micellar extraction is a promising liquid-liquid extraction technique that has the potential to be an alternative to other techniques due to its high efficiency and selectivity achieved in some systems [6].

Ionic surfactants adsorb onto metal oxides such as silica, alumina, ferric oxyhydroxide, and titanium dioxide, forming aggregates termed hemimicelles and admicelles, which can be used as sorbent materials in SPE. These aggregates consist of monolayers of surfactants adsorbing head down onto an oppositely charged surface (hemimicelles) and surfactant bilayers (admicelles). The process in which the analytes are partitioned between the bulk solution and these aggregates is referred to as adsolubilization, a phenomenon analogous to micellar solubilization in bulk aqueous solutions. Surfactant micelles are capable of increasing the solubility of most organic molecules in water. The mode by which the solubilization takes place is the attraction of the organic molecule into the surface of the micelle [7].

1.2 Background: the application of hemimicelle and admicelle in the analytical chemistry

Hemimicelles and admicelles are thoroughly investigated wonders in modern science. The definition of these terms is associated with the adsorption of micelles on surfaces. Fuerstenau in 1955 [8] discovered hemimicelles formations, which are surfactant monolayers adsorbed at the solid-solution interface and commonly understood to mean “head-on” formations. Whereas, admicelles are bilayer surfactant formations.

The charged block of ionic surfactants drawn to surfaces of opposite charge and surfactant chain–chain interactions result in these assemblies. A schematic of these structures are presented in Figure 1, and they can solubilize a wide spectrum of organic substances. The ability to solubilize substances in micelles is termed solubilization, and for admicelles and hemimicelles, the analogous term used is adsolubilization [9]. It is tempting to consider admicelle sorbents consisting of cationic surfactants coated on silica. In this case, for preconcentrating phenols, dihexadecyldimethyl ammonium hydroxide surfactants were coated on silica. It is worth noting that the reaction between the hydroxide ion of the surfactant and the weakly acidic phenols took place. As a result, this created an electrostatic hold between the cationic surfactant and the anionic phenolate analytes [9].

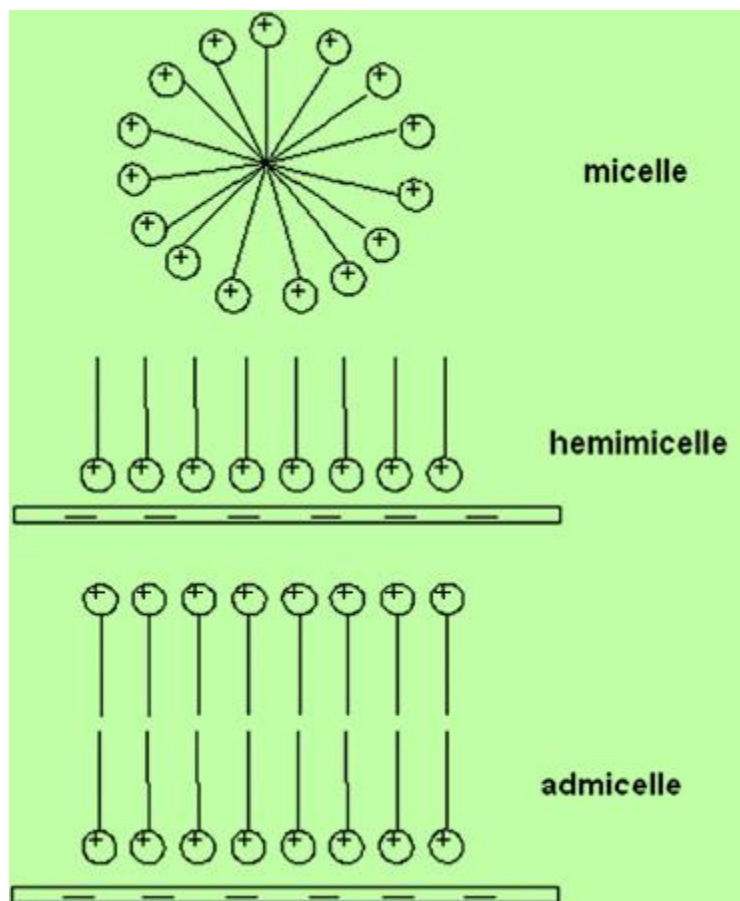


Figure 1. Micelle, hemimicelle, and admicelle structures in an aqueous solvent [9].

Solubilization is the process of including the solubilize onto or into micelles [9]. Solubilization may take place in a system having a solvent, an associated colloid, and a minimum of one other solubilize. The first part of the solubilization process is the breaking of the various kinds of intramolecular interactions between the components of the sample. These intrachains are Van der Waals forces, disulfide bonds, dipole-charge, hydrogen bonds, electrostatic interactions, dipole-dipole, and hydrophobic interactions. The second part of solubilization is the separation of the solvent's molecules to provide space in the solvent for the solute. The last step of solubilization is the interaction

between the solvent and the solute [9, 10]. A schematic of micellar solubilization of a fatty substance in water with the use of a dispersant is illustrated in Figure 2.

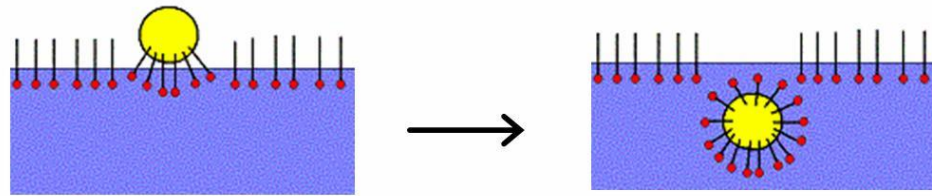


Figure 2. Schematic of micellar solubilization.

It is important to note that surfactants are amphiphilic molecules, meaning these molecules have a hydrophobic hydrocarbon tail and a hydrophilic polar head. At low volume concentrations, surfactant molecules are present in water as solvated monomers, but at higher concentrations, the hydrophilic polar heads will be on the outside of the micellar sphere while the hydrophobic tails will be aggregated into the core of micelles (Figure 3). Admicelle complexes are formed at surfactant concentrations below the critical micelle concentrations (CMC), but micelles are formed at surfactant concentrations above the CMC [9].

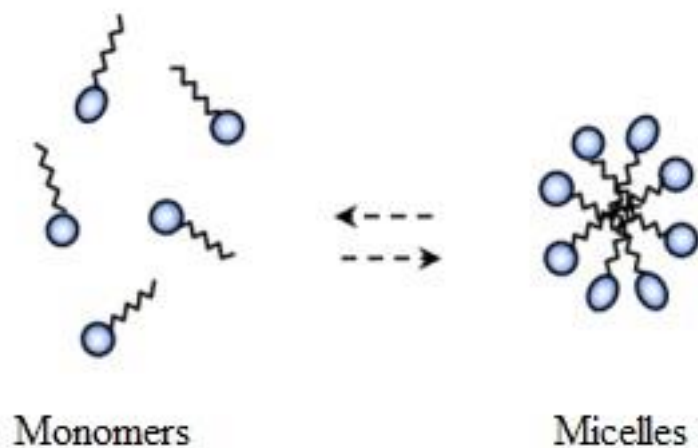


Figure 3. Surfactant molecules at low concentrations (monomers) and high concentration (micelles).

Hemimicelles or admicelles may form on surfaces depending on solution pH, the concentration of surfactant in solution, surface type, and electrolyte concentration [11]. The surface properties of the surfactant-coated particle are altered by the attached surfactant, and this quality can be used in the extraction of a specific analyte. These findings have been shown by Borge et al. [12]. The extraction of polyaromatic hydrocarbons [13], chlorophenols [14-16], and phthalates [17] with either a sodium dodecyl sulfate SDS- or dialkylsulfocuccinate-alumina sorbent have been presented. Dialkyl chained surfactant coating have greater hydrophobic properties than single chained SDS-coated alumina [17].

At present solid-phase extraction (SPE) is the most popular sample preparation method. It is used for concentrating, purifying, and separating of analytes. SPE is a method capable of separating compounds in a solution from other compounds according to their chemical and physical properties. SPE is used to separate analytes of interest from a general variety of assays, including blood, urine, soil, water, beverages, and

animal tissue. SPE is currently the most widely adopted method for enhancing low concentrations of constituents from a liquid solution [1].

It is of interest to consider the steps of SPE. A typical SPE consists of four basic steps: conditioning, loading, washing, and elution [1]. The equilibration of the cartridge with a slightly polar or non-polar solvent, which saturates the surface and permeates the bonded phase is the first stage. Then a buffer of the same composition as the sample is passed through the column to wet the silica surface. The sample is then introduced into the cartridge. As the sample passes through the stationary phase, the non-polar analytes in the sample will interact and retain on a non-polar sorbent while the solvent and other polar substances pass through the cartridge. After the sample is loaded, it is washed out with a polar solvent to remove interferences. The analyte is then removed with a non-polar solvent (Figure 4).

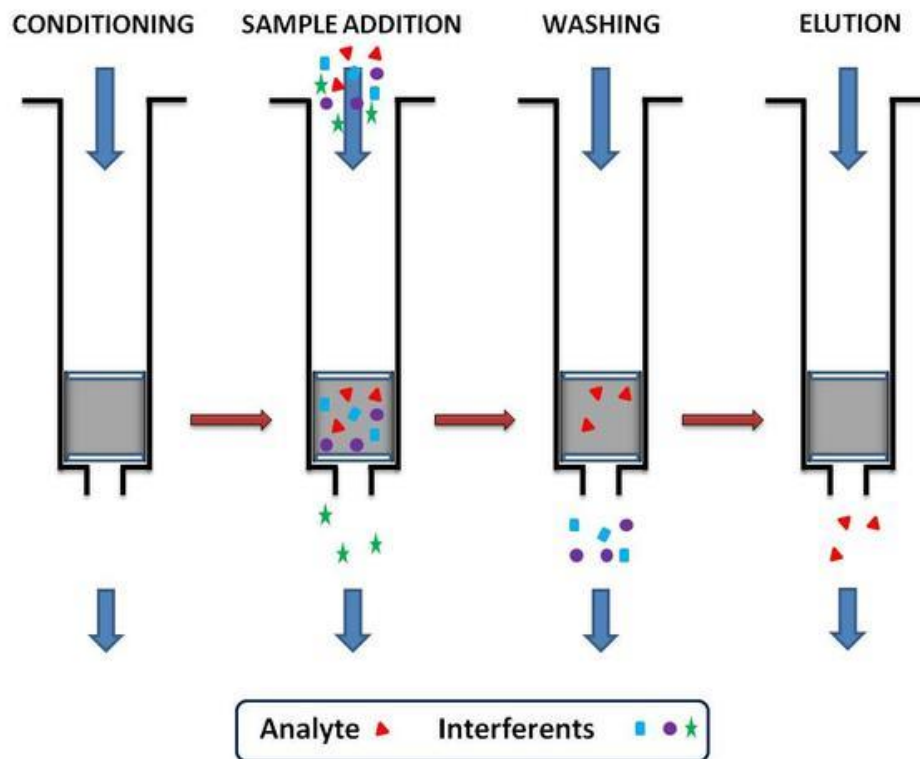


Figure 4. Stages of solid phase extraction (SPE).

A stationary phase of non-polar functionally bonded silica with small carbon chains often makes up the solid phase. This permanent phase will adsorb non-polar molecules, which can be collected with a non-polar solvent [1].

A great deal has been written about hemimicelles and admicelles of cetyltrimethylammonium bromide (CTAB) and cetylpyridinium chloride (CPC), adsorbed onto silica [18]. They are sorbents used for the SPE of linear alkylbenzenesulfonate. It has been established that the application of ammonium quaternary admicelles permits the use of hemimicelle/admicelle based SPE to the extraction of anionic solutes by electrostatic interactions. As a result, the extraction of aromatic compounds has become easier.

Mixed hemimicelle/admicelle adsorbents show great extraction efficiency for polycyclic aromatic hydrocarbons (PAHs) and good selectivity for natural organic substances. PAHs are regularly found together in groups of two or more. The linear alkyl benzenesulfonates (LAS) can form hemimicelles/micelles. SPE of PAHs was conducted by adding organic analytes and LAS through a column filled with 500 mg of eggshell membrane. Various factors were studied including LAS concentration, solution pH, ionic strength, and humic acid concentration on the effect of recoveries of PAHs. It is worth noting that LAS concentration and the pH of the solution had an important effect on extraction of PAHs, and the recovery of PAH compounds failed in the presence of salt and humic acids [19].

Pérez-Bendito et al. [20] reported that hemimicelles or admicelles of SDS on alumina and CTAB on silica were used for the concentration and purification of the estrogens estrone, 17 - beta-estradiol and ethynylestradiol. The cooperation between analyte-sorbent hydrophobic and cation- π interactions resulted in analyte retention. Parameters affecting the SPE of estrogens on both types of sorbents were examined. Adsolubilization was quantitative for SDS hemimicelles/admicelles and CTAB admicelles. The underlying assumption is that SDS hemimicelle-coated alumina was the selected sorbent due to the lower elution volume required and the higher sample flow rate permitted. The combination of estrogen adsolubilization-based SPE with liquid chromatography-diode array/fluorescence detection permitted the quantification of the target compounds from 20 to 100 ng/L. The authors asserted that the recovery for the estrogens in these environmental matrices (raw and treated sewage and river samples) was between 85 and 105% as well.

The more detailed discussion of this issue may be found in the works of Pérez-Bendito et al. in 2004 [7]. Their results established the suitability of surfactant-coated mineral oxides as sorbents for SPE of organic compounds. Their versatility for this application comes from the fact that different mechanisms of stabilization of analytes can be used, namely ion-exchange, hydrophobic interactions, ion-pair formation. The authors proved the suitability of admicelles to concentrate highly water-soluble organic ions from drinking water. It is worth noting that an on-line setup coupling of hemimicelle/admicelle-based SPE to LC can be used in any laboratory, and the regeneration of the sorbent can be achieved by removing the micellar aggregates with organic solvents or changing the pH. This way, a new sorbent can be prepared for every run. The micellar aggregates possess a dynamic nature. Therefore, special attention must be paid to method developments and optimization to achieve an accurate interpretation of the data obtained. In this context, guidelines can be established, as follows:

1. The effect of parameters affecting SPE (e.g. pH) on the surfactant adsorption isotherms must be known.
2. Partition constants of analytes will probably change the type or amount of sorbent, and because of this, the original parameters should be kept constant.
3. pH affects the charge density of the mineral oxide surface. For a fixed amount of mineral oxide, the amount of sorbent available for adsolubilization increases at determined pH values because the pH values affect the charge density of the mineral oxide surface.

Suen et al. [21] have proposed that strong cation exchange membranes, immobilized with octadecyltrimethylammonium hydroxide surfactants, have been successfully prepared and applied to the solid-phase extraction of phenolic compounds from water. The best surfactant immobilization procedure demands a HCl prewashing stage for activating the ion exchange groups. It has also been proposed to use a high surfactant feed amount. High enrichment factors and high recoveries were achieved if an aqueous alcohol solution was used as the eluent. These findings imply the entire process time is short, and the pressure drop is low. Therefore, this method is both time-saving and energy-saving. Moreover, scale-up can be easily achieved by stacking more membranes together without any deterioration in performance. In considering these factors, it is first important to highlight that hemimicellar/admicellar surfactant-immobilized membrane design may provide a beneficial alternative for preconcentrating hydrophobic components such as phenolic compounds.

The advantages of admicelle and hemimicelle SPE are:

1. High rates of absolute concentration for small sample volumes;
2. Low cost of analysis and absence of organic solvents;
3. Possibility of extraction of hydrophobic and hydrophilic analytes;
4. Environmental safety and inertness to biologically active substances;
5. The possibility of combining with physical and chemical methods of analysis.

The investigations of Suen et al. [22], include the immobilization of trimethylstearylammmonium hydroxide/methoxide surfactants onto two types of durable cation-exchange membranes. An important factor for the surfactant immobilization capacity was the cation-exchange capacity of the membranes. Also, the author stated that

a larger sample volume could be processed by using a membrane with a doubled cation-exchange capacity. The surfactant forming membrane had a hemimicellar, admicellar, or mixed structure and was controlled by the feed surfactant concentration. The author showed that membranes with 100% surfactant immobilization were used for the adsorption of phenolic compounds. In summary, this surfactant-immobilized membrane may be applied to the concentration of dilute hydrophobic analytes from water samples.

An important phenomenon in modern chemistry is the aggregation of surfactants at solid surfaces. Important factors include the surfactant molecular structure, hydrophilicity-hydrophobicity of the substrate surface, ionic strength, and the nature of the counter ion. It has long been known that the amount of charge the solid surface has a significant effect on the surface assembly of nonionic and ionic surfactants. Electrochemistry affords a great opportunity to research the effect of surface charge on the behavior of adsorbed surfactant molecules [23].

In the paper of J. Lipkowski et al. [24], dodecyl sulfate monolayers can be formed on gold surfaces by controlling surface potential. Controlling the potential of a gold surface results in different shapes and sizes of surfactant formations of DS. The author considered the potential controlled adsorption and aggregation of three prototypical surfactants on Au (111) surfaces in which surfactant had the same hydrocarbon tail length but different head groups. All three surfactants were controlled by the surface potential density of the electrode potential and the concentration of surfactant. It has been established that all three systems can form monolayers, which take place when there are small applied charge densities and surfactant concentrations less than $0.1C/C_{CMC}$. The monolayers consist of bilayers, which consist of two lines of molecules. The tails of

molecules in one line are oriented toward the tails of molecules in the second line, and the polar head groups are turned outward forming the rim of the molecular stripe. The structure is stabilized by Van der Waals, chain–chain, and chain–substrate interactions. It is important to note the initial adsorption stage is determined by the nature of the head group and the electrode’s crystallography. By increasing surfactant concentrations, these two-dimensional bilayers shape the formation of three-dimensional surface aggregates. Therefore, the nature of the head groups plays an important role, and different morphologies can be observed for different types of surfactant molecules. In the other hand, using Israelachvili’s packing parameter, the geometry of surfactant aggregates in the bulk solution can be predicted [25]. This parameter varies as a consequence of electrostatic interactions of the polar head with the charge at the electrode surface and as a result of co-adsorption of counter ions from the electrolyte [26, 27]. At the electrode surface, the packing parameter influenced by the charge or electrode potential, and the morphology of the surface aggregates changes upon adjustment of the electrical state of the metal. The authors have provided evidence of the electric field driven conversions of monolayers into hemicylindrical hemimicelles and changes between hemicylindrical structures into interdigitated bilayers and more multifarious composite structures.

The theoretical problems associated with the number of SDS molecules per unit cell of the long-range hemimicellar structure has been discussed [28]. The area of the unit cell of the two-dimensional lattice of hemimicellar SDS aggregates was equal to 206 \AA^2 . It was indicated that the adsorption isotherm for the limiting Gibbs excess of hemimicellar structure was $4.0 \times 10^{-10} \text{ mol/ cm}^2$. Using these data, the authors reported there were five SDS monomer units per unit cell. In the condensed state, the surface

concentration of SDS was doubled. Such a growth of the surface concentration of the surfactant proposes the opportunity of bilayer creation. It was observed that the hydrocarbon tails of the SDS molecules are tightly packed. A very high packing density of negatively charged molecules may be possible only if the charge of the anionic polar heads is well separated by the counter charge on the metal. Studies on the hemimicellar and condensed states have indicated that the main differences in the former, the force varies periodically in the direction parallel to the surface, reflecting periodicity of the hemimicellar structure, while in the latter, the force is uniform across the surface.

Previous research investigated the effect of changing SDS concentration on the capacitance [29]. These experiments revealed the formation of different surfactant layers relative to the change of SDS concentration. It was found that the lowest capacitance was achieved when 4 mM of SDS was used, while at higher SDS concentrations (greater than 4 mM), the capacitance of the gold electrode starts to increase. It was concluded that at a concentration of 4 mM SDS, a monolayer of DS surfactants (hemimicelle) was formed on the gold electrode and resulted in a drop in the surface capacitance. Also, at SDS concentrations greater than 4 mM (excess of SDS), a bilayer of DS surfactants (admicelle) was formed on the gold electrode which resulted in a gradual increase in the capacitance (Figure 5). In the hemimicelle formation, the hydrophobic portion (DS organic tail) faced the solution. In contrast, in the admicelle formation, the polar head (SO_4^-) faced the solution. However, various SDS concentrations (4, 6, 16, 32 mM) with 2 ppm 2-naphthol were investigated in this thesis work in the preconcentration experiments.

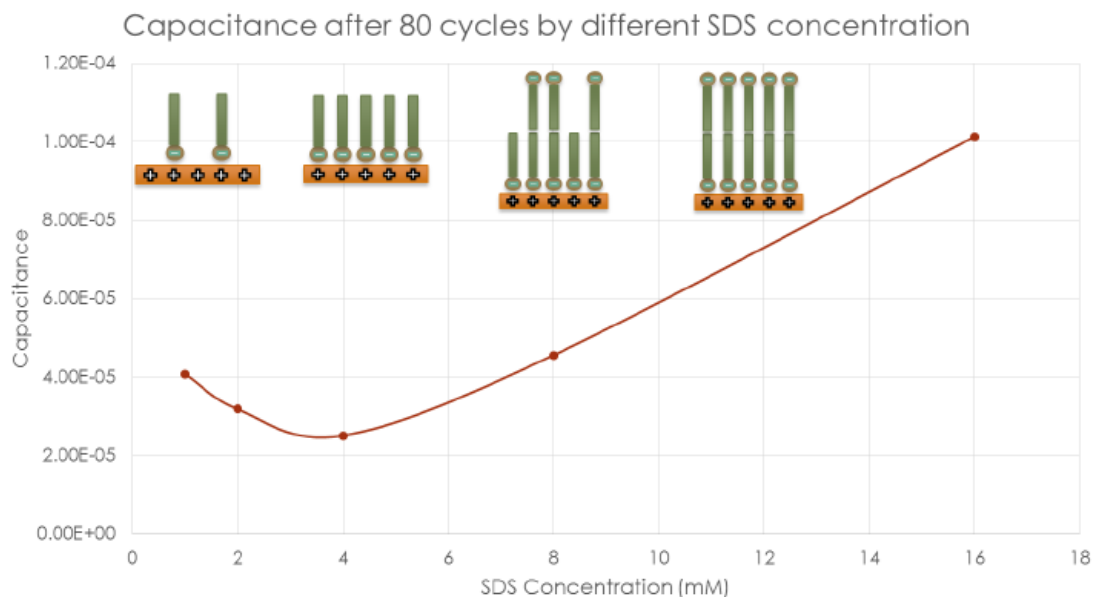


Figure 5. The capacitance measurement with different SDS concentrations after 80 cycles.

In this work, the investigation of the electrical control of DS surfactants on gold surfaces for analyte preconcentration prior chromatographic analysis step is presented. The formation of DS surfactant monolayer (hemimicelle) was exploited for analyte preconcentration. The aim was to use an applied potential of 0.6 V vs. Ag/AgCl for accomplishing the DS layer in the form of hemimicelle on the positively charged gold working electrode. Following by the absorption of 2-naphthol on the DS layer, based on the hydrophobic-hydrophobic interactions which can occur between the DS organic tail and the two benzene rings of 2-naphthol. Because the surfactant-analyte association is released by electrical control, organic solvents, which are used in conventional solid phase extraction, would be not required. Therefore, this procedure was predicted to be environmentally friendly.

2. Experimental part

Sodium dodecyl sulfate (SDS) and 2-naphthol were purchased from Sigma-Aldrich. 2-naphthol was used during this study because it has a similar chemical structure of the environmentally hazardous materials such as phenols and their derivatives. 2-naphthol is an organic compound that is composed of two aromatic rings, the hydrophobic portion, which facilitates its adsorption onto the DS surfactant layer, an –OH group at the 2-position, provides some hydrophilic properties giving 2-naphthol some water solubility (Figure 6). In addition, a SDS molecule consists of a carbon chain tail which is the hydrophobic part (*i.e.* non-polar), and the sulfate head which is the hydrophilic part (*i.e.* polar or charged). By having both of these properties, SDS is soluble in both water and non-polar organic solvent (Figure 7). During the DS surfactant layer formation, the attraction of the positively charged surface (gold surface) and the negative charge on the oxygen of the sulfate group, together with the chemical affinity of sulfate for gold, facilitate the formation of the DS monolayer on gold.

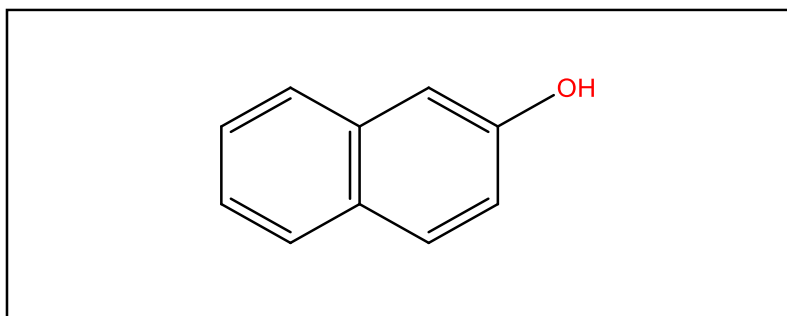


Figure 6. The chemical structure of 2-naphthol.

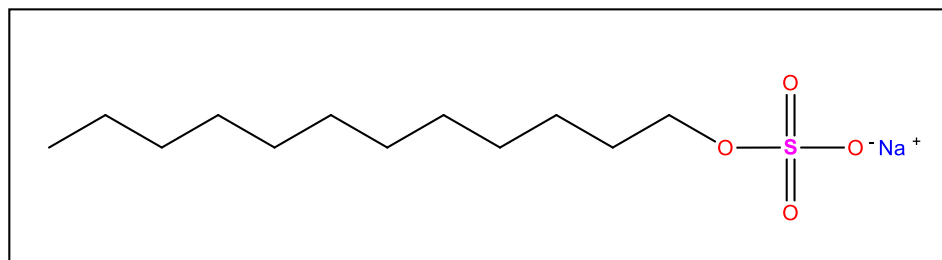


Figure 7. The chemical structure of Sodium dodecyl sulfate (SDS).

2.1 Standard solutions

All the chemicals were of analytical reagent grade. First, a stock solution of 100 ppm 2-naphthol was prepared by dissolving 0.025 g in 250 mL of de-ionized water. In addition, 32 mM of SDS was prepared by dissolving 4.614 g in 500 mL of de-ionized water. A stock solution of 100 mM sodium sulfate was prepared by dissolving 0.7102 g in 50 mL of de-ionized water. The working standard solutions of 2 ppm 2-naphthol, (4 mM, 6 mM, & 16 mM) of SDS, and 1 mM of Na_2SO_4 were prepared daily from the stock standard solutions.

2.2 Major instrumentations and materials were used

Impedance spectroscopy measurements were made using a model PARSTAT 2263 (Princeton Applied Research). A nickel gold-coated column was constructed to investigate the DS surfactant monolayer formation on a gold surface. For the electrochemical step, the gold substrate was connected to the working electrode through a Pt wire, while another Pt wire served as the counter electrode, and an Ag/AgCl (saturated KCl) electrode served as the reference electrode. All scanning electron microscope images were taken with a Scanning Electron Microscope (SEM) (JSM-6510LV with a LAB6 Gun) in the Biology Department of Western Kentucky University. The high performance liquid chromatograph (HPLC) was composed of a 9012 pump, a C8 column,

and two different detectors: a Prostar 330 PDA detector, and a Prostar 363 fluorescence detector, all from Varian. The mobile phase was a mixture of HPLC grade methanol and water in a 70:30 ratio and was pumped at a rate of 0.5 mL/min for 10 minutes for 2-naphthol and 15 minutes for anthracene. For detection, the wavelength range of the photodiode array detector was set from 200 nm to 400 nm with a monitored wavelength of 250 nm, while the excitation-emission wavelengths of the fluorescence detector were set at 350 nm and 400 nm respectively. The nickel gold-coated column was constructed using a 50 mL test tube; Teflon parts; aluminum parts; O-ring; Teflon tubing; a glass bar which helps divert the solution toward the wall of the column; and 10 nickel gold-coated pieces ($3 \times 4 \text{ cm}^2$) were rolled and placed at the bottom of the column (Figure 8, and 9).

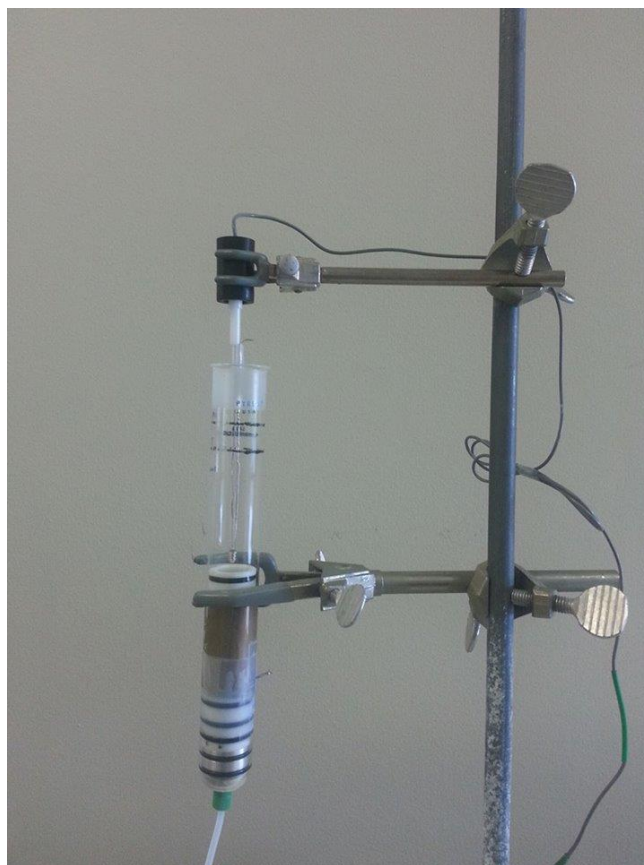


Figure 8. Nickel gold-coated column.



Figure 9. Nickel gold-coated pieces (3 x 4 cm²).

2.3 Capacitance measurements for monitoring the formation of DS monolayer on positively charged gold substrates

Gold slides were purchased from Evaporated Metal Films Corporation. The slides have a dimension of 25 mm x 75 mm x 1 mm with 50 Å Ti initially coated on the glass and a 1000 Å Au layer evaporated on top of the Ti layer. Electrochemical Impedance Spectroscopy (EIS) has been performed using a PARSTAT 2263 (Princeton Applied Research) for the investigation of the DS surfactant monolayer formation on the gold surface. A 5-mL electrochemical cell was used to allow solution contact with the gold slide. Multiple cyclic voltammetry (CV) scans were used to clean the gold surface. Five mL of a cleaning solution, which consisted of 0.1 M sulfuric acid (H₂SO₄) and 5 mM potassium chloride (KCl), were spiked into the cell. The cleaning procedure using this solution involved three stages. The first stage was performed by running 10 CV cycles from 0.2 V to 0.9 V, the second stage was performed by running 10 CV cycles from 0.2 V to 1.2 V, and the third stage was performed by running 10 CV cycles from 0.2 V to 1.5 V. After that, the experiment was directed over three stages. The blank stage was

performed by loading 5 mL of 1 mM Na₂SO₄ as a supporting electrolyte into the electrochemical cell, and then 50 capacitance cycles were taken at 0.6 V vs. Ag/AgCl; then the cell was turned off. Next, the SDS stage was performed by loading 5 mL of 4 mM SDS prepared with 1 mM Na₂SO₄, then 50 capacitance cycles were taken at 0.6 V vs. Ag/AgCl. Next, the cell was kept on, and the SDS solution was exchanged with 1 mM Na₂SO₄ solution. Finally, the 2-naphthol stage was performed by introducing a cell concentration of 2 ppm 2-naphthol and then 50 capacitance cycles were taken at 0.6 V vs. Ag/AgCl.

2.4 The column procedure involving three steps

2.4.1 The control experiment

This experiment was conducted to monitor whether there is a reduction of 2-naphthol concentration with the absence of both an electric field and SDS. 40 mL of 2 ppm 2-naphthol was added into the column. A 60-mL syringe pump, which was purchased from Fisher Scientific, was used manually in a continuous back and forth motion for 4-5 minutes to mix the solution in and out of the column. An aliquot was taken and injected into the HPLC for 2-naphthol peak area determination. Due to a consistent residual volume of water that remains between the gold substrates, a sample was taken at the beginning of each stage to measure the change in 2-naphthol concentration. Afterward, the column was cleaned with 50% methanol and rinsed with de-ionized water 6-8 times to remove traces of methanol.

2.4.2 The electric field blank experiment

The same setup that was performed in step 1 was used except that potential of 0.6 V vs. Ag/AgCl was applied during the 45 minutes to create an electric field at the surface of the electrode. This experiment was conducted to monitor whether there is a reduction in 2-naphthol concentration in the presence of the electric field and in the absence of SDS. First, a solution of 2 ppm 2-naphthol and 1 mM Na₂SO₄ was prepared in 40 mL of de-ionized water and spiked into the column. From this test, a sample of 2-naphthol was taken and injected into the HPLC to determine the 2-naphthol cell concentration before the application of an electric field. A potential of 0.6 V vs. Ag/AgCl was then applied to the gold working electrode for 45 minutes. While the cell was on, an aliquot of the solution containing 2-naphthol solution was taken and injected into the HPLC for the 2-naphthol peak area determination. Also, the same experiment was conducted using an applied potential of 0.8 V vs. Ag/AgCl. In addition, two other types of supporting electrolytes (1 mM of KNO₃, 1 mM of sodium phosphate buffer of pH7) and plain water were used to investigate the effect of changing electrolytes on the 2-naphthol concentration.

2.4.3 Preconcentration experiment

This experiment involved three stages: DS layer formation, extraction, and releasing of 2-naphthol. First, 40 mL of 4 mM SDS was prepared in 1 mM Na₂SO₄ and loaded into the column. Next, the syringe pump was used manually in a continuous back-and-forth motion, prior to the application of the electric field, to remove the bubbles produced during the loading of SDS solution and to make sure that no bubbles remain between the gold substrates. Next, 0.6V vs. Ag/AgCl was applied to the gold working

electrode for 50 capacitance cycles which last for 45 minutes (1 cycle/0.9 min). At this point, the negatively charged DS surfactant (the oxygen in sulfate group of DS surfactant) was attracted to the positively charged surface (gold substrate) and a DS surfactant monolayer formed. After 45 minutes of delay time, the SDS solution was exchanged with 1 mM Na₂SO₄ solution to remove the excess SDS (unbound to the gold). This process was performed using a 60-mL syringe to remove the solution from the top of the column and exchange it with 1 mM Na₂SO₄ solution multiple times. Afterward, while the cell was on, 800 μ L of 100 ppm 2-naphthol was spiked into the column, and the volume was diluted to 40 mL to provide a solution concentration of 2 ppm 2-naphthol. Next, the solution mixture was left for 45 minutes to reach an equilibrium condition and for 2-naphthol to be adsorbed onto the DS surfactant monolayer. When the extraction stage was finished, an aliquot of the solution containing 2-naphthol solution was taken while the cell was on and injected into the HPLC for 2-naphthol peak area determination. Next, the releasing stage involved applying a negative potential of -0.6 V vs. Ag/AgCl to the gold working electrode and then turning the cell off to remove both the DS layer and the adsorbed 2-naphthol. Another sample of the solution containing 2-naphthol solution was taken while the cell was off and injected into the HPLC for monitoring the gradual change in 2-naphthol concentration. Finally, the solution was completely drained out of the column, and 10 mL of 70% methanol was added. The solution was then mixed multiple times using a syringe pump. An aliquot of this solution was taken and injected into the HPLC for 2-naphthol peak area determination. The same experiment was performed using various SDS concentrations: 6 mM, 16 mM, and 32 mM.

2.5 Anthracene control experiment

100 ppm of anthracene stock solution was prepared in HPLC grade methanol by adding 0.01 g of anthracene to 100 mL of the solvent. Because the solubility of the anthracene in water is very low, 0.04 ppm anthracene aqueous stock solution was prepared in 1 L of de-ionized water. In addition, the working standard solution of 0.01 ppm anthracene was prepared daily from the aqueous stock solution of 0.04 ppm. However, because the column was made of Teflon tubing components (hydrophobic material), anthracene, which is a hydrophobic molecule, was attracted to these hydrophobic sites, and therefore the column was not used in this step. Instead, a 300-mL glass beaker was used to monitor the adsorption of anthracene on gold substrates. First, 10 nickel gold-coated pieces ($3 \times 4 \text{ cm}^2$) were placed in the beaker. Next, 300 mL of 0.01 ppm anthracene was prepared and loaded into the beaker. Then, a glass stirrer was used for mixing the solution for 2 hours. Additionally, an aliquot of the solution containing anthracene solution was taken and injected into the HPLC every 10 minutes to monitor the gradual decrease in anthracene solution concentration. Next, 200 mL of 70 % methanol (HPLC grade) was prepared and used as a rinsing solution. Finally, the 10 nickel gold-coated pieces were rinsed four times (50 mL each) then an aliquot of this solution was injected into the HPLC each time to determine how much anthracene was adsorbed onto the gold substrates. Likewise, the same procedure was performed with 10 bare nickel pieces "uncoated nickel" ($3 \times 4 \text{ cm}^2$) to monitor the adsorption of anthracene on nickel for comparison with nickel gold-coated experiment. In these two experiments, mass balance measurements were used to account for all of the anthracene (solution and surface bound).

2.6 9-anthracenecarboxylic acid control experiment

100 ppm of the 9-anthracenecarboxylic acid stock solution was prepared in HPLC grade methanol by adding 0.01 g of 9-anthracenecarboxylic acid to 100 mL of the solvent. Because the solubility of the 9-anthracenecarboxylic acid in water is very low, 0.04 ppm 9-anthracenecarboxylic acid aqueous stock solution was prepared in 1 L of de-ionized water. In addition, the working standard solution of 0.01 ppm 9-anthracenecarboxylic acid was prepared daily from the aqueous stock solution of 0.04 ppm. As discussed before in the anthracene control experiment procedure, the column was not used in this step. Instead, a 300-mL glass beaker was used to monitor the adsorption of 9-anthracenecarboxylic acid on gold substrates. First, 10 nickel gold-coated pieces ($3 \times 4 \text{ cm}^2$) were placed in the beaker. Next, 300 mL of 0.01 ppm 9-anthracenecarboxylic acid were prepared and loaded into the beaker. Then, a glass stirrer was used for mixing the solution for 2 hours. Additionally, an aliquot of the solution containing 9-anthracenecarboxylic acid solution was taken and injected into the HPLC every 20 minutes to monitor the gradual decrease in 9-anthracenecarboxylic acid solution concentration. Next, 200 mL of 70 % methanol (HPLC grade) was prepared and used as a rinsing solution. The 10 nickel gold-coated pieces were rinsed four times (50 mL each) then an aliquot of this solution was injected into the HPLC each time to determine how much 9-anthracenecarboxylic acid was adsorbed onto the gold substrates. Finally, mass balance measurements were used to account for all of the 9-anthracenecarboxylic acid (solution and surface bound).

2.7 Micro-Lab techniques for gold deposition on Monel alloy

2.7.1 Cleaning procedure

Careful preparation was necessary for proper bonding of gold to the base metal. Gold chloride is less tolerant of impurities than that of cyanide baths. This sensitivity to impurities was observed as deposition on the substrate in various oxidation states and colloidal formation during electroplating in either a rose or deep purple color. Placement of the anode was also very important; this influenced the plating patterns and the quality of gold coating observed on the substrate material. Ultimately, this resulted in the development of a bath apparatus with a platinum electrode capable of encompassing the substrate metal by 360 degrees.

The Monel alloy was selected first for this project. In this section, the preparation processes and the performance characteristics discovered during the electrochemical experiments were covered. Monel is an alloy of nickel and copper in which both metals are soluble in any proportion; this is known as a solid solution alloy. This alloy is highly resistant to corrosion and was selected for this project for that reason. The Monel's strong resistance to corrosion required a relatively strong chemical activation before the gold would permanently bond to the alloy. Traditional chemical activation methods were unsuccessful (usually a 50 % HCl solution at approximately 45-50° C). Details of the preparation and activating, as well as the electrodeposition process are discussed in the next section.

HCl was obtained from Fisher Scientific, gold chloride solution was obtained from Sigma-Aldrich, and electrochemical cleaning powder "ElectrokingTM" was obtained from Gold Touch Inc. The Monel utilized in this experiment was a woven wire cloth. The

wire diameter was approximately 33 μm and the pore area (size) was approximately $60.0 \times 10^{-6} \text{ m}^2$. The pore size was not consistently distributed throughout the surface of the woven mesh. All SEM images were taken with the SEM (JSM-6510LV with a LAB6 Gun) in the Biology Department of Western Kentucky University. Once the Monel was the desired shape, it was washed using cleaning solution (Sparkleen) and rinsed in de-ionized water. The Monel was then placed in a 95 - 100° C degreasing bath containing Electroking™ at a concentration of 1.0 gram Electroking™ to 100 mL de-ionized water. The mesh plates were degreased for 45-60 minutes. The plates were then rinsed in nano-pure water. Once rinsed thoroughly, the woven mesh plates were stored in nano-pure water, which was purged with argon at a continuous rate of 0.1 cfm.

2.7.2 Activation Solutions and plating procedure

Activation solution was prepared by adding 25 mL concentrated nitric acid, 75 mL glacial acetic acid, and 1.5 mL of HCl to a Pyrex beaker. All the solutions were obtained from Fisher Scientific. The solution temperature was consistent at 25° C. The activation solution consists of the fully concentrated acids mixed at their respective ratios and so must be confined to a vent hood at all times. The plating procedure was conducted in a 100-mL beaker as a reaction cell containing 30 mL of 5.88 mM of HAuCl_4 gold chloride, 10 mL of 0.15 M of HCl "gold bath solution" and 60 mL of de-ionized water. The solution was circulated with a 0.5 cm magnetic stir bar rotating at 160 rpm. The plating tank was fully assembled and securely positioned for magnetic stirring. Once the apparatus was secured, the DC power supply (preset to 5.4 V DC) was connected, and plating solution was then added. Once activation and plating solutions were prepared, the Monel mesh was removed from the argon purged nano-pure water. Next, the Monel plate

was pre-connected to a platinum wire to serve as a working electrode (cathode) and dipped for 3 seconds in the activation solution, and another platinum wire was coiled and placed in the 100-mL beaker (reaction cell) to serve as a counter electrode (anode). The Monel was then removed and rinsed with nano-pure water completely and immediately immersed into the gold bath. Plating was continued until a complete uniform gold coating was observed. The plated Monel was then removed from the bath and rinsed with nano-pure water and gently dried with purified air. Finally, SEM images were taken for both uncoated Monel and Monel-coated gold for further surface analysis.

2.8 The process of Nickel coated with Gold

The nickel mesh that was used for gold plating was obtained from Dexmet. The pore size of nickel mesh was $6.4 \times 10^{-4} \text{ cm}^2$. The plating procedure was conducted in a 100-mL beaker as a reaction cell containing a solution of 5.88 mM of HAuCl_4 gold chloride and 0.15 M HCl "gold bath solution" mixed in a ratio of 3:1.

The nickel sheet was cut into 10 nickel pieces ($3 \times 4 \text{ cm}^2$). Then, 5 g of the cleaning powder "ElectrokingTM" were dissolved in 500 mL of de-ionized water. Next, the ten nickel plates were placed in the cleaning solution and stirred and heated to the boiling point for 3 hours. Afterward, the nickel plates were rinsed with de-ionized water multiple times and then sonicated in methanol for 15 minutes using an ultrasonic cleaner (3510 Branson). Then, the ten nickel plates were dried at 40°C for 5 minutes. An activation solution of 50:50 hydrochloric acid and water was prepared to remove the oxide layer on nickel surface and make the nickel surface more active and ready for gold deposition. The temperature of the activation solution was maintained at $60\text{--}70^\circ \text{C}$. A nickel piece was connected to a platinum wire to serve as a working electrode (cathode),

and another platinum wire was coiled and placed in the 100-mL beaker (reaction cell) to serve as a counter electrode (anode). The nickel piece was then immersed into the activation solution for 2 minutes (bubbles formation on nickel surface is a good indicator that the cleaning of nickel surface takes place). 0.5 V was used for the gold plating procedure. After that, the nickel piece was placed into the plating solution (a ratio 3:1 of a mixture of 5.88 mM of HAuCl_4 and 0.15 M of HCl) for about 2 minutes. Next, the nickel piece was air dried. Then, a quick wiping test was performed using a tape to make sure the coated gold did not come off easily. Furthermore, SEM images were taken for both bare nickel and nickel-coated gold for further surface analysis.

3. Results and discussion

3.1 Capacitance measurements for monitoring the formation of DS monolayer on positively charged gold substrates

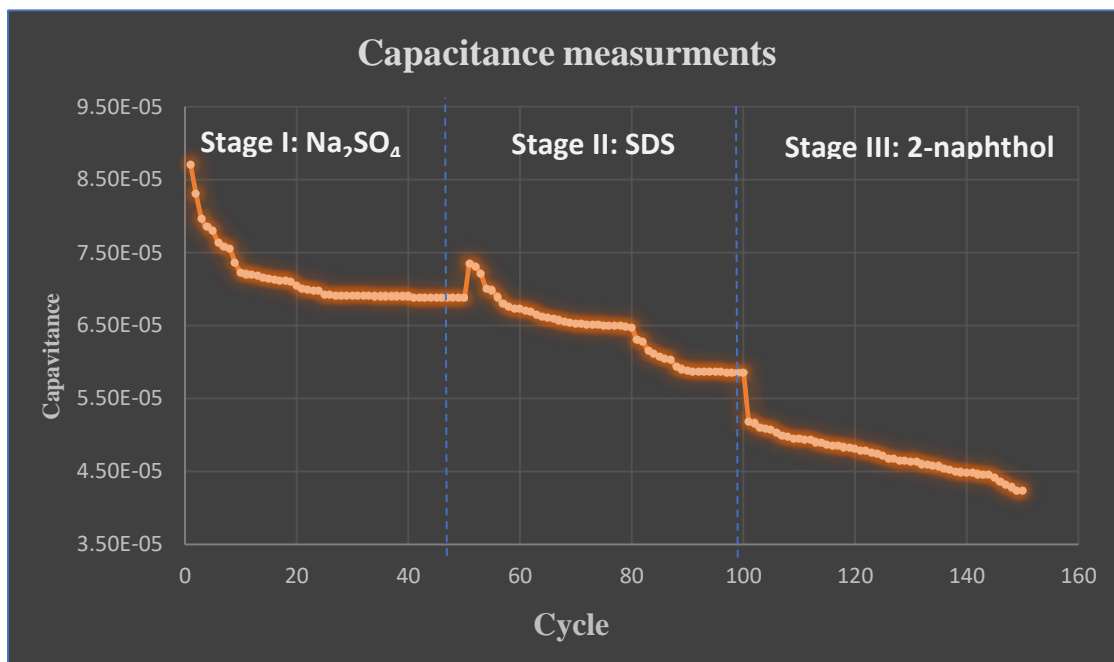


Figure 10. Capacitance measurements at three different stages: Stage I: 1 mM Na₂SO₄; Stage II: 4 mM SDS in 1 mM Na₂SO₄; Stage III: 2ppm 2-naphthol in 1 mM Na₂SO₄.

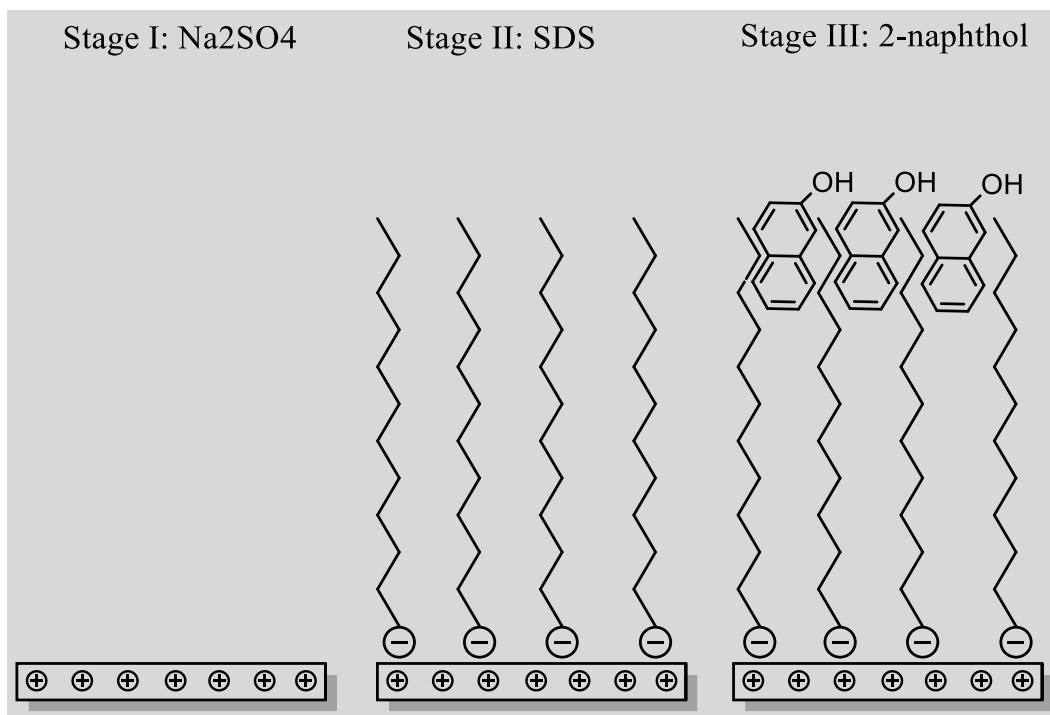


Figure 11. Schematic representation of the capacitance measurements that shown in Figure 10.

As shown in Figure 10 and 11, three capacitance stages were performed at an applied 0.6 V vs. Ag/AgCl using a 5-mL electrochemical cell, a gold slide (planar gold as working electrode), a platinum wire as a counter electrode, and a Ag/AgCl / (saturated KCl) electrode served as the reference electrode. The purpose of these experiments is to see the changes in capacitance values when a new layer formed on the gold surface. The first 25 cycles (22.5 minutes; 1/0.9 cycle/min) of each stage are the time required for the solution to reach an equilibrium. It was found that the initial capacitance of the gold surface dropped after each stage, and this was attributed to the presence of a new layer formed on the gold surface. First, stage I is the blank capacitance measurement of gold with 1 mM Na₂SO₄ (supporting electrolyte), these capacitance measurements were

conducted to monitor the change in the capacitance values and were compared with next two stages. Then, after the first 50 cycles (Na_2SO_4 stage), the cell was turned off and rinsed with de-ionized water multiple times, then 5 mL of 4 mM SDS solution prepared in 1 mM of Na_2SO_4 was loaded into the cell. Stage II is the "SDS stage". The aim was to get a DS surfactant monolayer formed on the gold surface. The drop in capacitance values in the second stage revealed the formation of the DS surfactant monolayer on the gold surface. At this point, the polar head (SO_4^-) of the DS was attracted to the positively charged gold surface, and DS's organic tail, facing the solution, resulted in dropping in capacitance. Whereas, the increase in the capacitance measurement at the beginning of this stage "SDS stage" was due to the time required for the system to reach equilibrium. Lastly, stage III "2-naphthol stage", 2 ppm 2-naphthol was spiked with 1 mM Na_2SO_4 while the cell was on. In this stage, further reduction in the capacitance was observed and was attributed to the adsorption of 2-naphthol onto DS surfactant monolayer.

3.2 The column procedure

In order to get the DS surfactant monolayer formed onto the gold surface, our electrical impedance spectroscopy (EIS) instrument was used by applying a positive charge (0.6 V vs. Ag/AgCl) on the working electrode. The working electrode was a porous nickel mesh obtain from Dexmet and was cut into ten square pieces ($3 \times 4 \text{ cm}^2$) and coated with gold. These ten square pieces were coiled and placed into the column to provide a surface area about 245.5 cm^2 . This porous gold surface provides a larger surface area than planar surfaces. However, with this design (10 pieces were put one upon another in coiled form), it was difficult to monitor capacitances due to a more

complex porous surface. However, HPLC was used to monitor the change in 2-naphthol concentration.

3.2.1 The control experiment

The procedure of a control test (step 1) involved the analysis of two samples: First, a premixed sample was taken after loading 40 mL of 2 ppm 2-naphthol and mixing with syringe pump one time. It was found that there was about 6 - 12% drop in 2-naphthol concentration due to the consistent residual volume of water that remains between the gold substrates after each experiment. Another sample was taken after 4 -5 minutes of mixing to observe any further reduction in 2-naphthol concentration. It was found that there was almost no significant change in 2-naphthol concentration (Figure 12). It could be concluded that there was no significant reduction caused by the column components. However, the majority of the drop in 2-naphthol concentration was due to a dilution resulting from the residual volume of water (3-4 mL) that was left after every experiment.

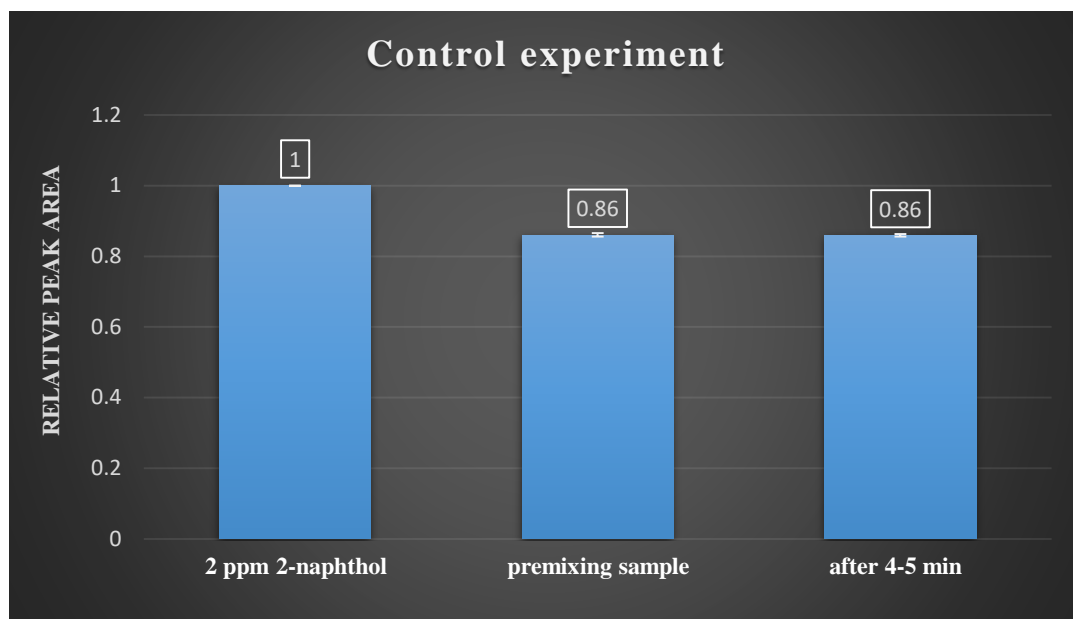


Figure 12. The differences in peak areas for three samples: 2 ppm 2-naphthol, 2-naphthol (premixing sample), 2-naphthol after 4-5 min of mixing.

3.2.2 The electric field blank experiment

Step2: in this experiment, 0.6 V was applied to the gold working electrode in the absence of SDS to monitor the change in 2-naphthol concentration in the presence of the electric field. The investigation of other variables that might result in decreasing in 2-naphthol concentration was conducted. One way to achieve this was to see whether the applied potential is destroying 2-naphthol or causing 2-naphthol to be adsorbed onto the gold surface. The same setup that was used in the control test experiment was performed in this step, except for the presence of the electric field. The experiment began using 2 ppm 2-naphthol solution prepared in 1 mM of Na_2SO_4 . First, 0.6 V vs. Ag/AgCl was applied to the gold working electrode for 45 minutes. Then, an aliquot of the solution containing 2-naphthol solution was taken while the cell was on and injected into the HPLC for 2-naphthol peak area determination. The peak area of the 2-naphthol was

compared to the one taken during the control test experiment and they were statistically the same. Higher voltages are to be avoided because the aromatic compounds with hydroxyl functional groups start oxidizing at 0.7 V [30]. To prove this hypothesis, the same experiment was performed at an applied potential of 0.8 V vs. Ag/AgCl using 40 mL of 2 ppm 2-naphthol prepared in 1 mM of Na_2SO_4 with the same column setup. Next, 0.8 V vs. Ag/AgCl was applied to the gold working electrode for 45 minutes. After 45 minutes of the applied potential, there was about 20% decrease in 2-naphthol concentration under 0.8 V of applied potential. However, it could be concluded that the potential being applied at 0.6 V for 45 minutes was not destroying 2-naphthol or causing the 2-naphthol to be adsorbed onto the gold surface (Figure 13). Contrarily, the potential being applied at 0.8 V for 45 minutes resulted in about 20% decrease in 2-naphthol concentration (Figure 14). Moreover, two other types of supporting electrolytes and water (1 mM KNO_3 and 1mM sodium phosphate buffer of pH7) were used in this step at 0.6 V of applied potential to investigate the effect of using other electrolytes. However, as shown in Figure 15, changing the supporting electrolyte had no significant effect on 2-naphthol concentration. KNO_3 is a good supporting electrolyte but in this case, it was not used, because it was observed when adding KNO_3 to SDS solution, at higher concentrations of KNO_3 , this caused SDS to precipitate. However, these observations were not noticed with the other supporting electrolytes.

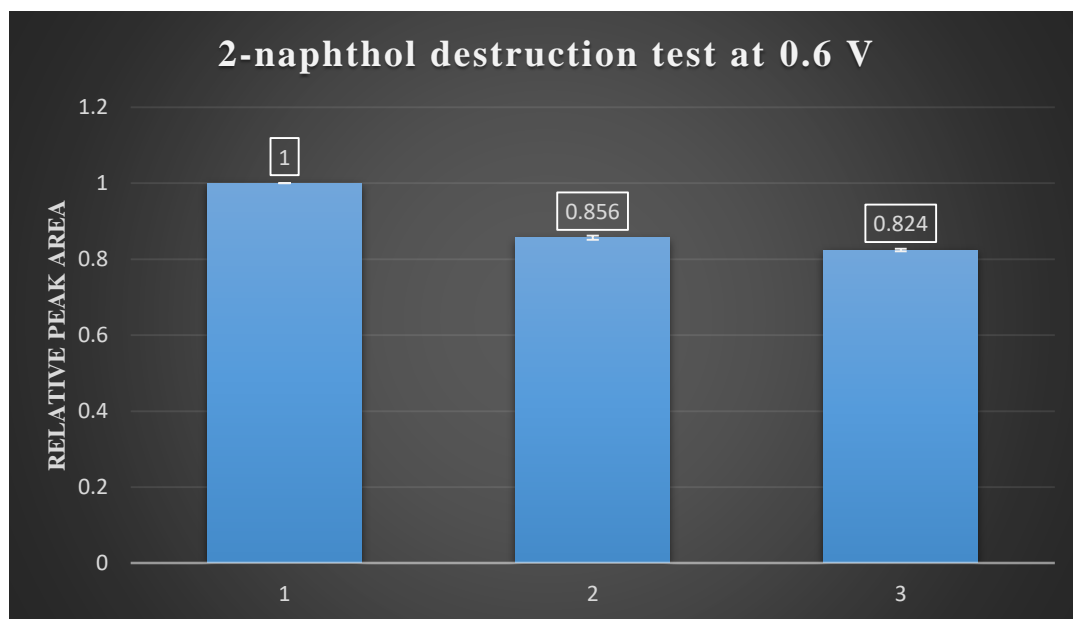


Figure 13. 2-naphthol destruction test: 1: 2 ppm of 2-naphthol, 2: 2-naphthol with no potential applied, 3: 2-naphthol at 0.6 V for 45 minutes.

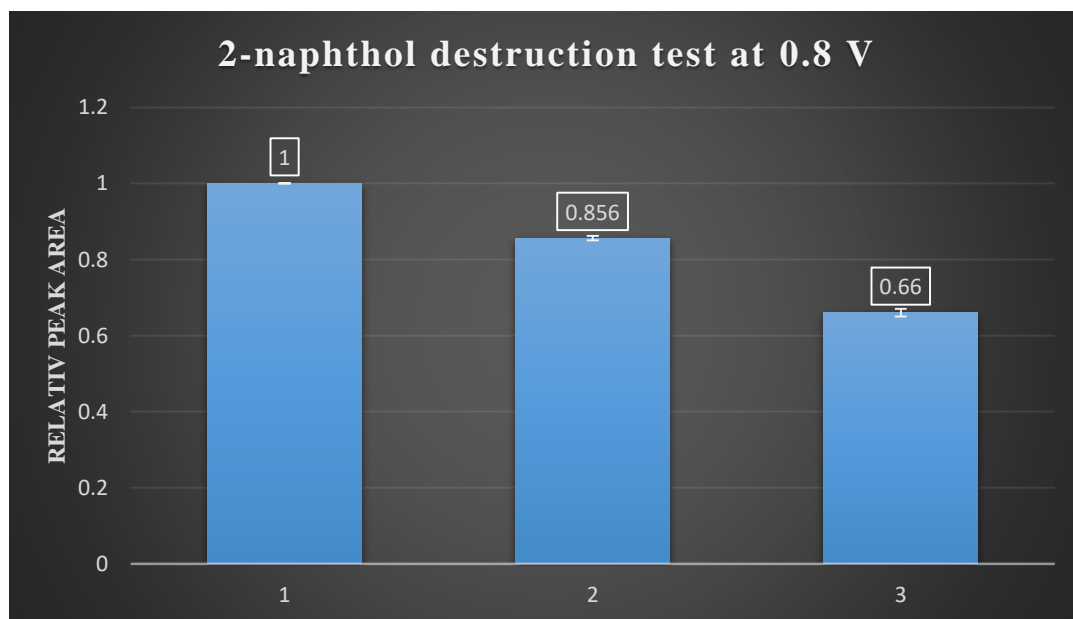


Figure 14. 2-naphthol destruction test: 1: 2 ppm 2-naphthol, 2: 2-naphthol with no potential applied, 3: 2-naphthol at 0.8 V for 45 minutes.

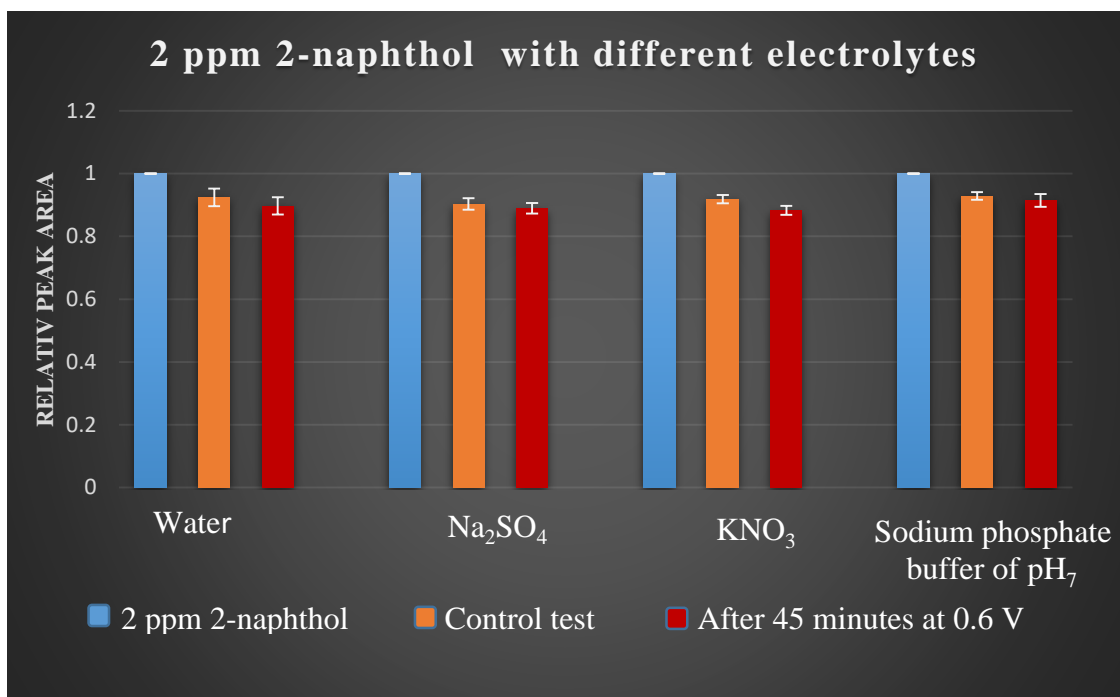


Figure 15. The effect of using different electrolytes on 2-naphthol concentration with an applied potential of 0.6 V vs. Ag/AgCl.

3.2.3 Preconcentration experiment

The aim of this experiment was to achieve DS surfactant monolayer formation via the attraction of the polar site of the DS “sulfate group” to the net positively charged gold substrates. As described previously, the DS layer may extract and preconcentrate 2-naphthol via hydrophobic interactions that occur between the side chain of hydrocarbon tail and the 2-naphthol aromatic rings (Figure 16).

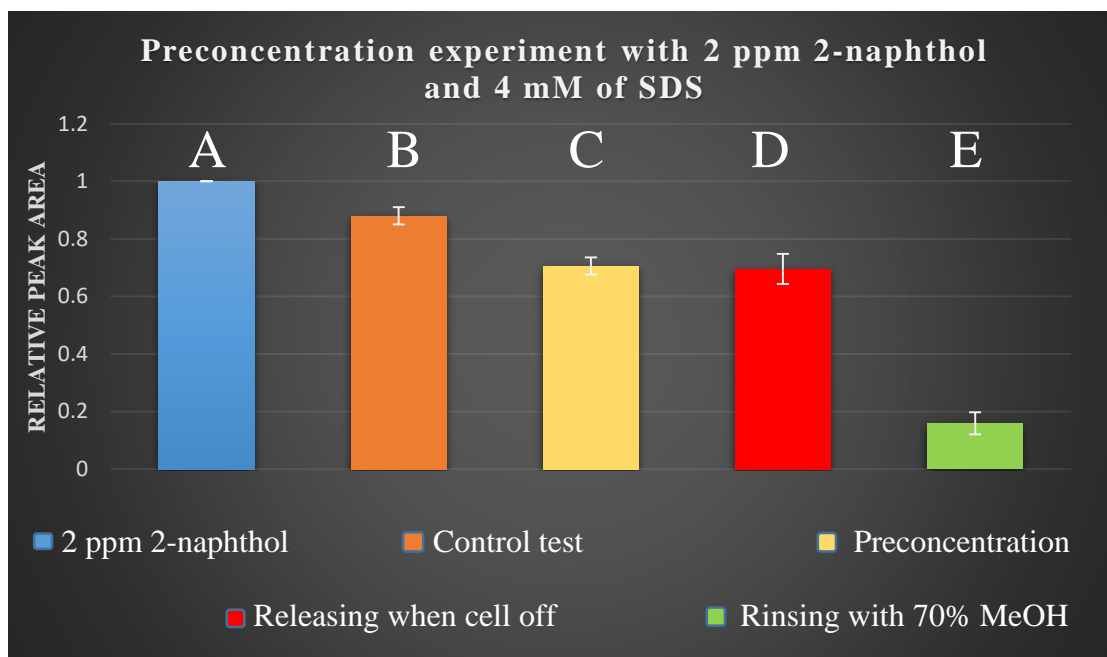


Figure 16. The preconcentration experiment of 2 ppm 2-naphthol and 4 mM SDS at 0.6 V vs. Ag/AgCl; where A: 2 ppm of 2-naphthol, B: Control test, C: Preconcentration at an applied potential of 0.6 V, D: Releasing stage when the cell was turned off, and E: Rinsing with 10 mL of 70% methanol.

Firstly, the preconcentration procedure was performed with 2 ppm 2-naphthol and 4 mM SDS at 0.6 V vs. Ag/AgCl. In comparison to the initial concentration of 2 ppm 2-naphthol at the beginning of this experiment, there was a 12% drop in 2-naphthol concentration from stage A to Stage B which was due to the residual volume of water that was left after each experiment (discussed earlier). Also, as discussed earlier, there was almost no significant change in 2-naphthol concentration (less than 2%) in the presence of the electric field at 0.6 V. Meanwhile, after 45 minutes at this applied potential, there was a 20% drop in 2-naphthol concentration at the extraction stage C compared to the previous stage B. This drop was attributed to the adsorption of 2-naphthol onto the DS surfactant monolayer which was already being formed via the attractive forces that

occurred between the positively charged gold surface and the negatively charged DS. However, stage D involved no change in 2-naphthol concentration after applying -0.6 V vs. Ag/AgCl to the gold working electrode and turning the cell off. Next, the solution was completely drained out of the column. Next, 10 mL of 70% methanol was used to remove the remaining amount of 2-naphthol that was trapped between the gold substrates during the preconcentration stage C. It was found that about 20% of the 2-naphthol was trapped between the gold substrates which was the same amount of 2-naphthol that was lost during the preconcentration stage C.

Furthermore, another preconcentration experiment was performed using 2 ppm 2-naphthol and 6 mM SDS at an applied potential of 0.6 V vs. Ag/AgCl to see whether the increase of SDS concentration would improve the formation of the DS surfactant monolayer on the gold working electrode as well as increase the adsorption of 2-naphthol on DS surfactant monolayer. It was found that increasing the SDS concentration did not improve the DS surfactant monolayer formation nor 2-naphthol adsorption (Figure 17). Nevertheless, another two preconcentration experiments were performed using surfactant concentration above the CMC, 16 mM and 32 mM SDS at an applied potential of 0.6 V vs. Ag/AgCl. No improvement was observed. However, this may be because the DS layer is not stable enough to hold much of the analyte, 2-naphthol. In other words, the binding strength of the negatively charged surfactants to the positively charged gold surface is not strong enough to be used as a solid phase system for analyte preconcentration. Burgess et al. reported the standard free energies for this system. They calculated the Gibbs energy of the SDS adsorption is -40 kJ/mol. This suggests that SDS is weakly chemisorbed to the Au (111) substrates [28].

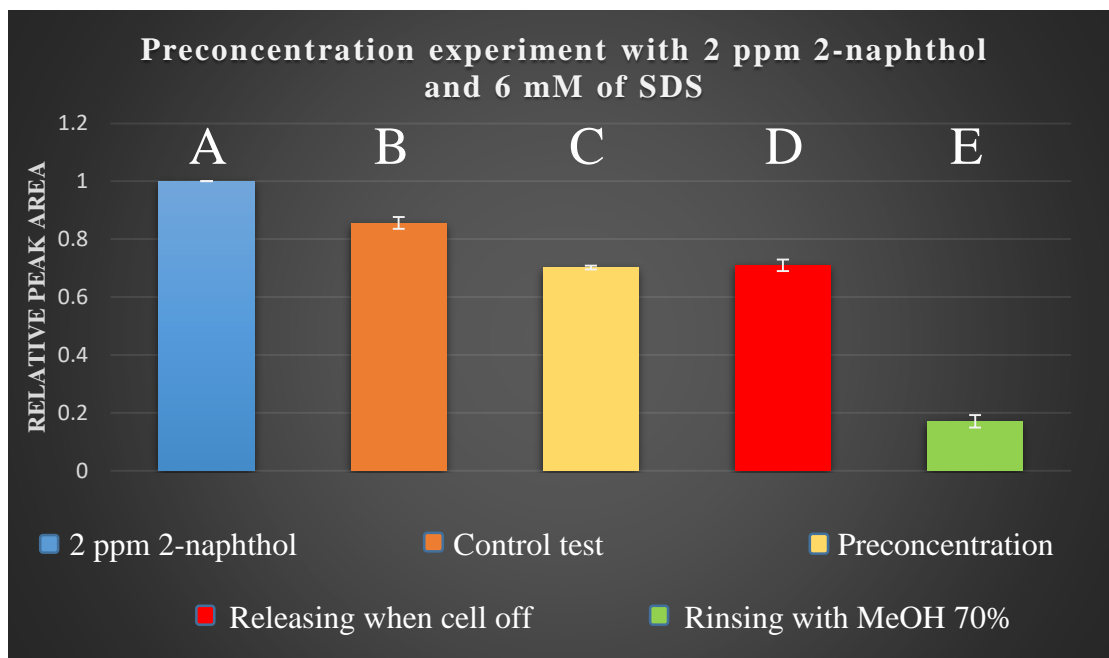


Figure 17. The preconcentration experiment of 2 ppm 2-naphthol and 6 mM SDS at 0.6 V vs. Ag/AgCl; where A: 2 ppm of 2-naphthol, B: Control test, C: Preconcentration at an applied potential of 0.6 V, D: Releasing stage when the cell was turned off, and E: Rinsing with 10 mL of 70% methanol.

3.3 Anthracene control experiment

Anthracene was used as a substituted test molecule instead of 2-naphthol because anthracene has no functional group that is easily oxidized (anthracene is more hydrophobic than 2-naphthol). Therefore it may be possible to increase the potential applied to the gold working electrode and see how this would improve the DS surfactant monolayer. A working standard solution of 0.01 ppm anthracene was prepared from the aqueous stock solution of 0.04 ppm anthracene and added to a 300-mL beaker contained 10 nickel gold-coated pieces ($3 \times 4 \text{ cm}^2$). An aliquot of the solution containing anthracene solution was taken and injected into the HPLC every 10 minutes during a two-hour test.

However, it was found that after two hours, almost all the anthracene was adsorbed onto the gold substrates (Figure 18). The reason behind this phenomenon is that the outer electrons for noble metals such as gold and silver experience s-d orbital hybridization which increases the mobility of these electrons and make them more active and also facilitates the formation of chemical bonds between noble metals and the target analyte, anthracene. Next, nickel gold-coated plates were rinsed four times with a total of 200 mL of 70:30 methanol and water (each rinse 50 mL) and an aliquot of this solution was injected into the HPLC after each rinse for the determination of bound anthracene concentration. Next, mass balance measurements were performed to calculate the amount of anthracene that was recovered and compared to the starting amount of the anthracene at the beginning of this experiment. Almost all of the anthracene about 96%, which was adsorbed onto the gold substrates was successfully recovered (Figure 19). The propagation of error for this measurement ranged from 1-4%.

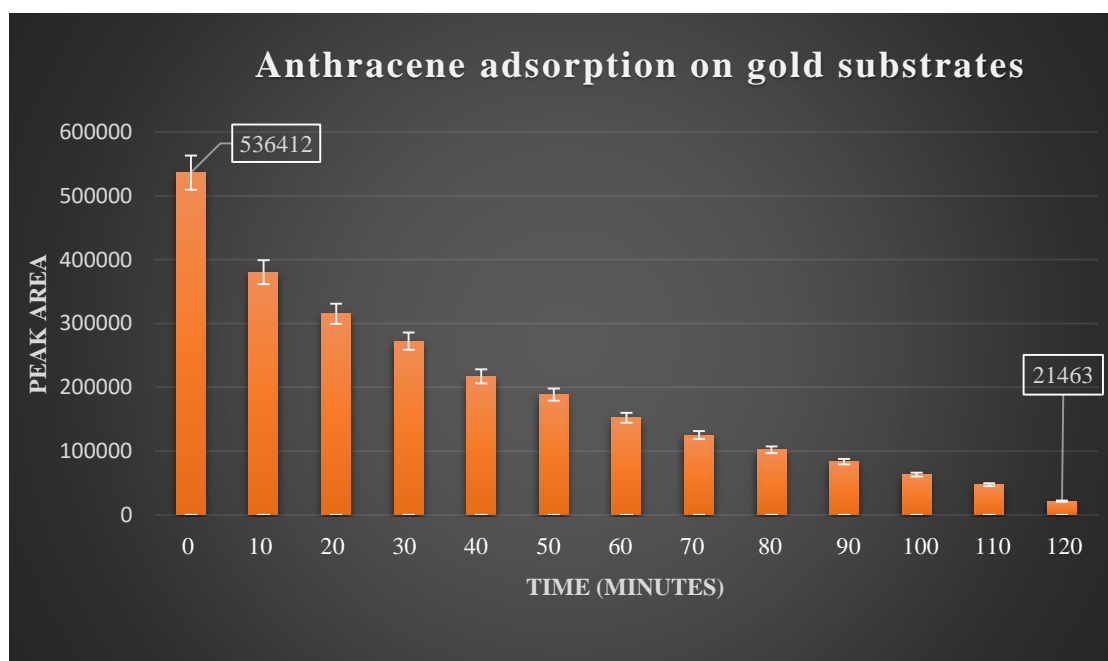


Figure 18. Anthracene adsorption onto gold substrates during the two-hour test.

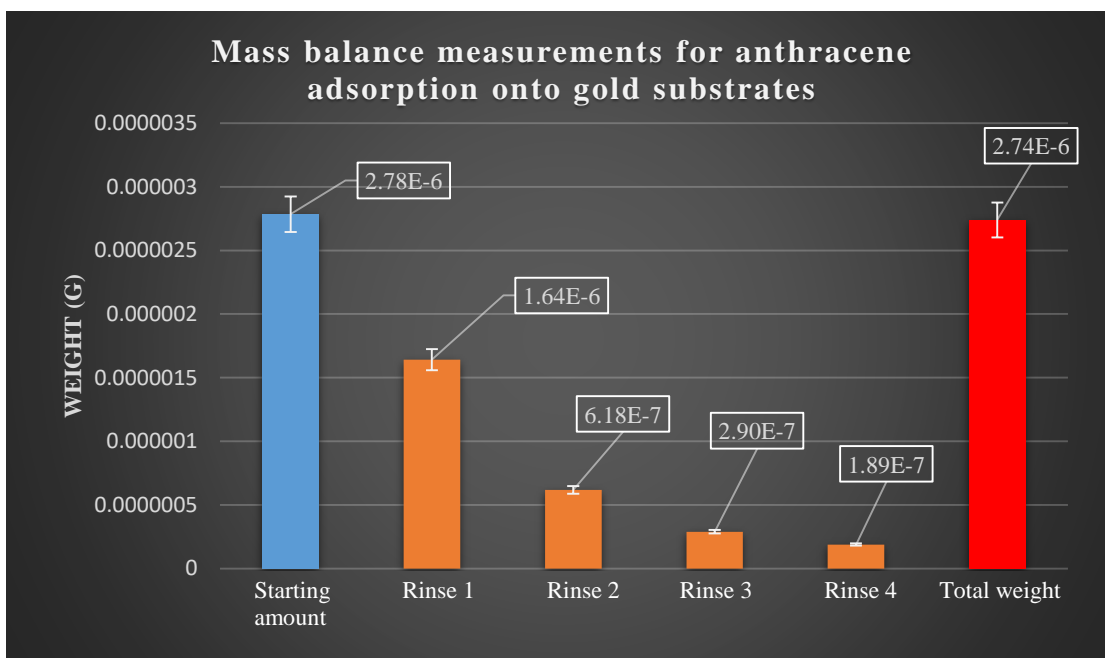


Figure 19. Mass balance measurements for anthracene adsorption onto gold substrates.

The same procedure was performed with 10 bare nickel pieces "uncoated nickel" ($3 \times 4 \text{ cm}^2$) to monitor the adsorption of anthracene on bare nickel and was compared to the previous experiment using nickel coated with gold. An aliquot of the solution containing anthracene solution was taken and injected into the HPLC every 10 minutes during a two-hour test. However, as shown in Figure 20, it was found that after two hours, there was only 25% drop in anthracene concentration due to the adsorption of anthracene onto nickel substrates. Next, the anthracene was rinsed four times from nickel plates with a total of 80 mL of 70:30 methanol and water (each time 20 mL), then an aliquot of this solution was injected into the HPLC for the determination of anthracene concentration. As noticed in this experiment, instead of using 200 mL, 80 mL were used to rinse the anthracene which was adsorbed onto nickel. Because only 25% of anthracene was adsorbed onto nickel, and anthracene was not sticking to the nickel as strongly as to

the gold substrates, so there was no need to use a large volume to recover the adsorbed anthracene from the nickel substrates. Next, mass balance measurements were performed to calculate the amount of anthracene that was recovered and compared to the starting amount of the anthracene at the beginning of this experiment. All the anthracene (about 25% of the original), which was adsorbed onto the nickel substrates, was successfully recovered (Figure 21). The propagation of error for this measurement ranged from 1-4%. As a consequence, from these anthracene adsorption experiments with either gold or nickel substrates, it could be concluded that anthracene cannot be used for the purpose of this thesis's analyte preconcentration concept because it adsorbs well to the gold without applying potential.

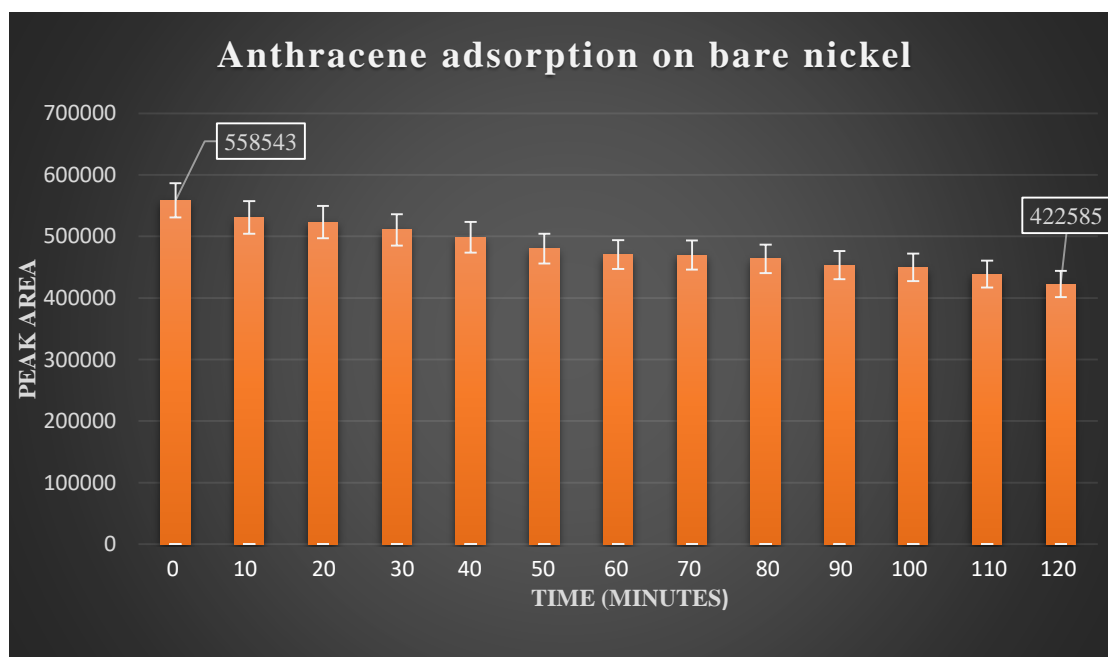


Figure 20. Anthracene adsorption onto nickel substrates during the two-hour test.

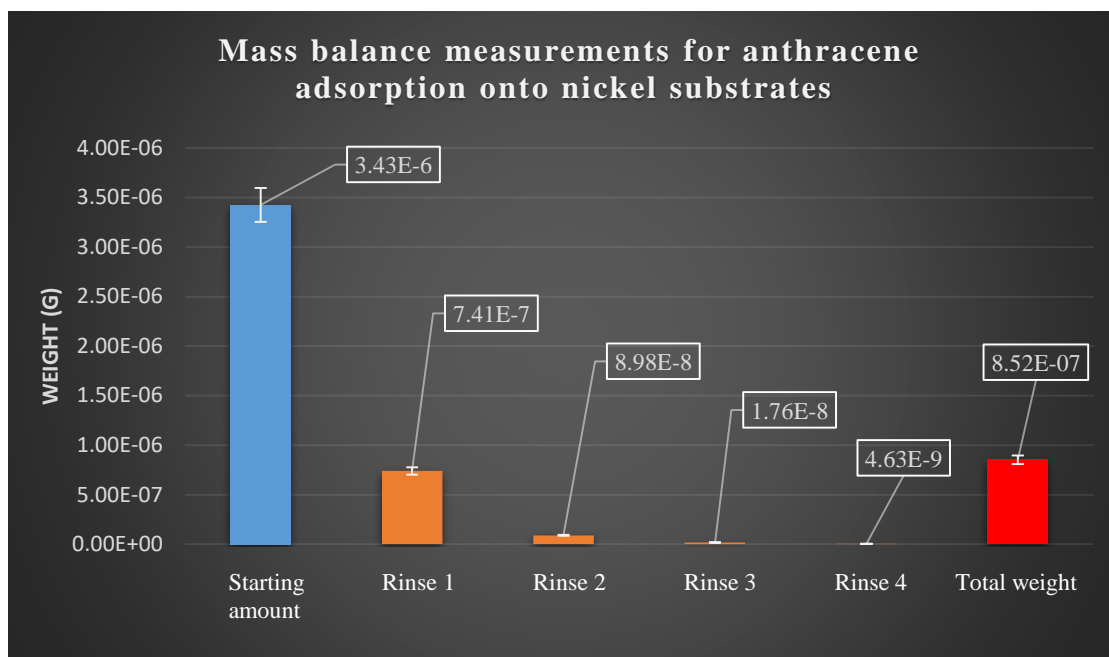


Figure 21. Mass balance measurements for anthracene adsorption onto nickel substrates.

3.4 9-Anthracenecarboxylic acid control experiment

In addition to anthracene, 9-anthracenecarboxylic acid was also used as a substituted test molecule instead of 2-naphthol to see the effect of the carboxylic acid group at position 9 on its adsorption on gold substrates and compare it to the adsorption of anthracene on gold substrates. A working standard solution of 0.01 ppm 9-anthracenecarboxylic acid was prepared from the aqueous stock solution of 0.04 ppm 9-anthracenecarboxylic acid. An aliquot of the solution containing 9-anthracenecarboxylic acid solution was taken and injected into the HPLC every 20 minutes during a two-hour test. However, it was found that after two hours about 51% of 9-anthracenecarboxylic acid was adsorbed onto the gold substrates (Figure 22). Compared to the anthracene (about 96% adsorbed), 9-anthracenecarboxylic acid has less affinity to the gold substrates due to the existence of -COOH group at position 9 which changes the electron density of 9-anthracenecarboxylic acid and results in less adsorption on the gold substrates. Next,

the 9-anthracenecarboxylic acid was rinsed from nickel gold-coated plates four times with a total of 200 mL of 70:30 methanol and water (each rinse 50 mL) then an aliquot of this solution was injected into the HPLC after each rinse for the determination of 9-anthracenecarboxylic acid concentration. Next, mass balance measurements were performed to calculate the amount of 9-anthracenecarboxylic acid that was recovered and compared to the starting amount of the 9-anthracenecarboxylic acid at the beginning of this experiment. It could be said that all the 9-anthracenecarboxylic acid about 51%, which was adsorbed onto the gold substrates, was successfully recovered (Figure 23). The propagation of error for this measurement ranged from 1-4%.

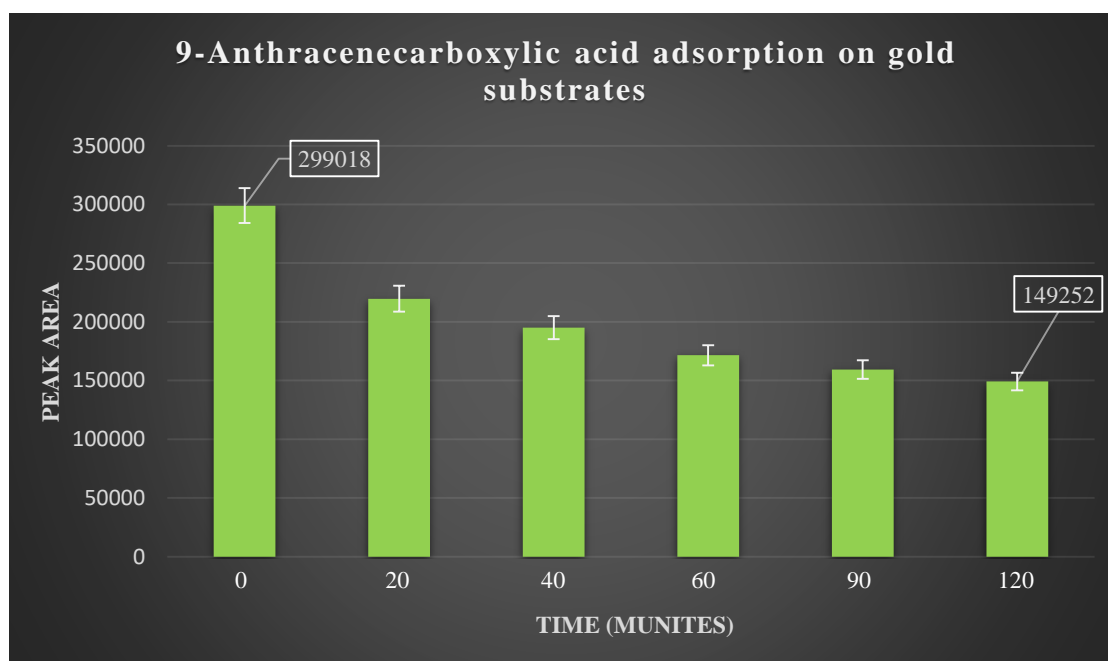


Figure 22. 9-anthracenecarboxylic acid adsorption onto gold substrates during the two-hour test.

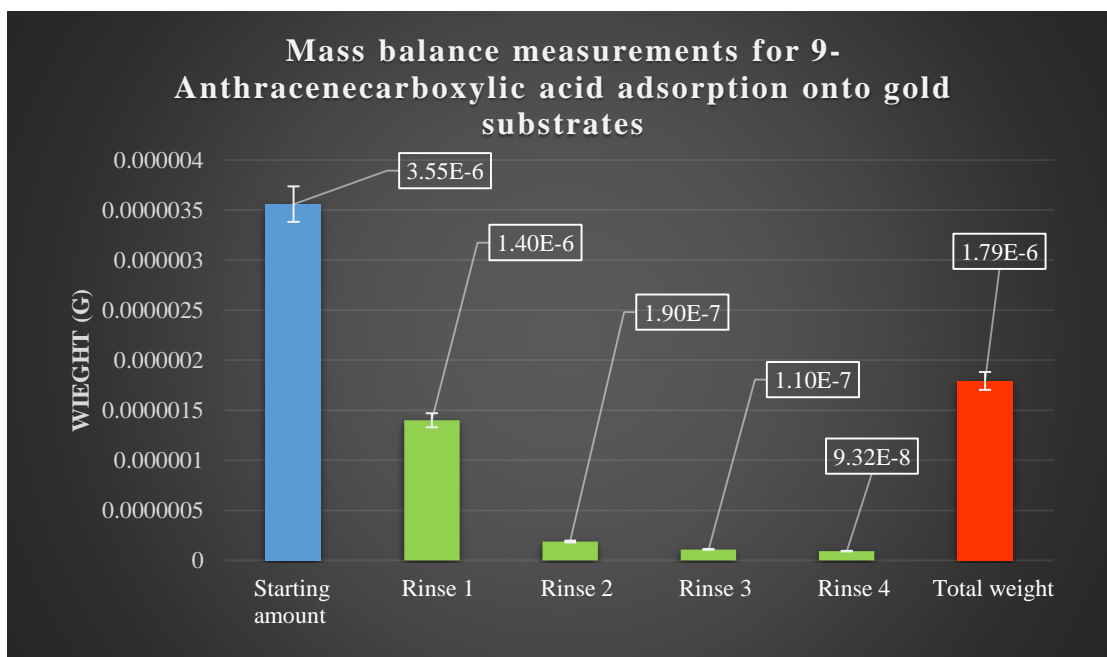


Figure 23. Mass balance measurements for 9-anthracenecarboxylic acid adsorption onto gold substrates.

3.5 The process of Monel coated with Gold: scanning electron microscope SEM images

Activation of the Monel surface required a trial and error approach due to the very corrosive nature of the activation solution. Figure 24 illustrates the aftereffect of overexposure for 5 seconds to the activation solution when referenced to the new material (Inactivated Monel alloy). The left side of Figure 25 illustrates the corrosive nature of the activation solution. It was found that a five-second exposure resulted in a dramatic loss of surface area of the Monel alloy. In contrast, as shown in the right side of Figure 25, three consecutive immersions that lasted a total of 3 seconds were successful to remove the oxides from the surface of the Monel mesh. When this referenced to a new inactivated Monel alloy (Figure 26), a three-second activation method is sufficient enough to remove the oxide for electrodeposition and still preserve the surface area of the Monel alloy

substrate. However, it should be noted that there is less cross section of the Monel alloy wire after activation. Calculations indicate a reduction in wire diameter by approximately 2.4×10^{-5} m via studies with SEM

Successful electrodeposition of gold on Monel alloy is illustrated in Figure 27. In SEM studies Monel gold-coated returns a higher signal and brightness than that of the original alloy. Wire diameter comparisons between plated and unplated material indicate a larger diameter wire on the gold plated material; this suggests restoration of the wire's original diameter in addition to a slight increase resulting from the gold deposition. It should be noted, however, that Figure 27 could be misleading from a straightforward interpretation, this is due to the high signal return from the gold. Less shadowing is observed in the Monel gold-coated, so the edges of the wire are more pronounced and defined. The uncoated Monel alloy has more shadowing due to a lower return signal, so the outside edge of the wire boundary is more obscured limiting the observations to a more qualitative nature than quantitative. However, elemental analysis was performed for the two spots which are marked as area 1 (un-coated Monel alloy) and as area 2 (Monel gold-coated) in Figure 27. In Figure 28, the elemental analysis for area 1 represents a higher nickel abundance. Higher gold abundance was observed from area 2 due to the existence of a gold layer on Monel alloy. Activation solutions consisting primarily of HCl were unsuccessful in properly preparing the substrate for electrodeposition of gold. Concentration ranges of HCl were evaluated at 50%, 80%, and concentrated. Results of this activation and plating process produced lustrous, but very fragile plating that would rub off of the Monel with the most delicate of touch. This was sufficient evidence to prove failed chemical activation of the Monel substrate. This also suggested that the gold

layer was formed via the nucleation–coalescence mechanism due to improper bonding to the Monel substrate. SEM analysis was not conducted on the specimens in which plating was unsuccessful.

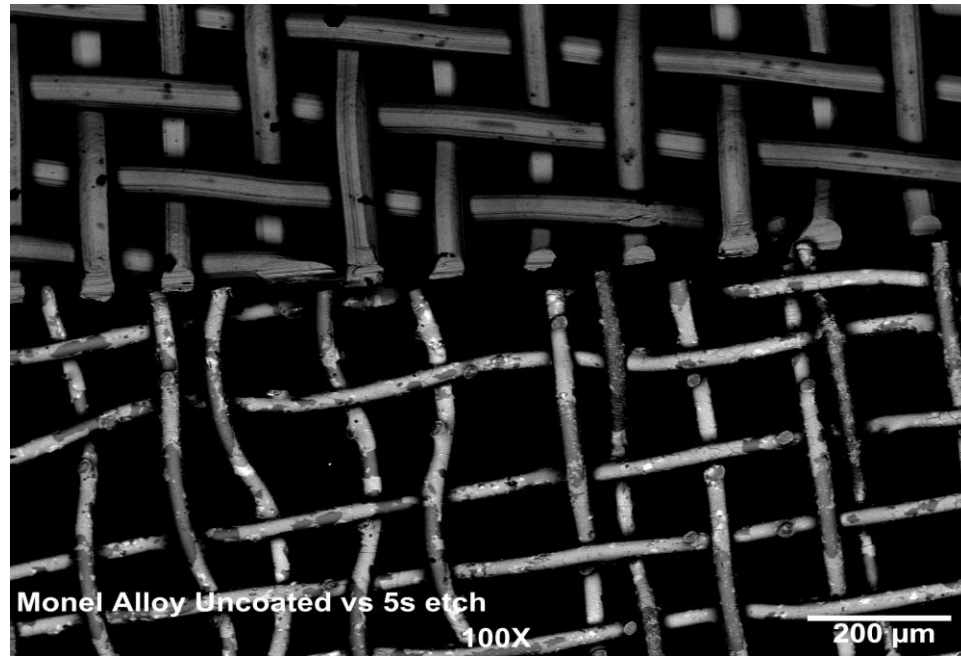


Figure 24. Inactivated Monel and overexposure to the activation solution.

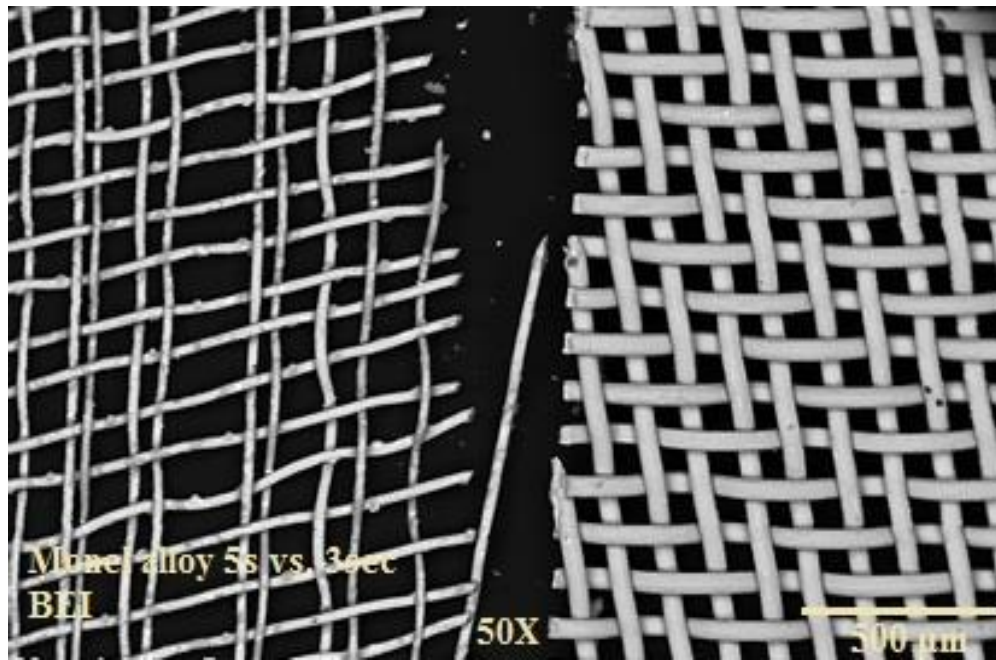


Figure 25. Monel alloy emersion time in activation solution.

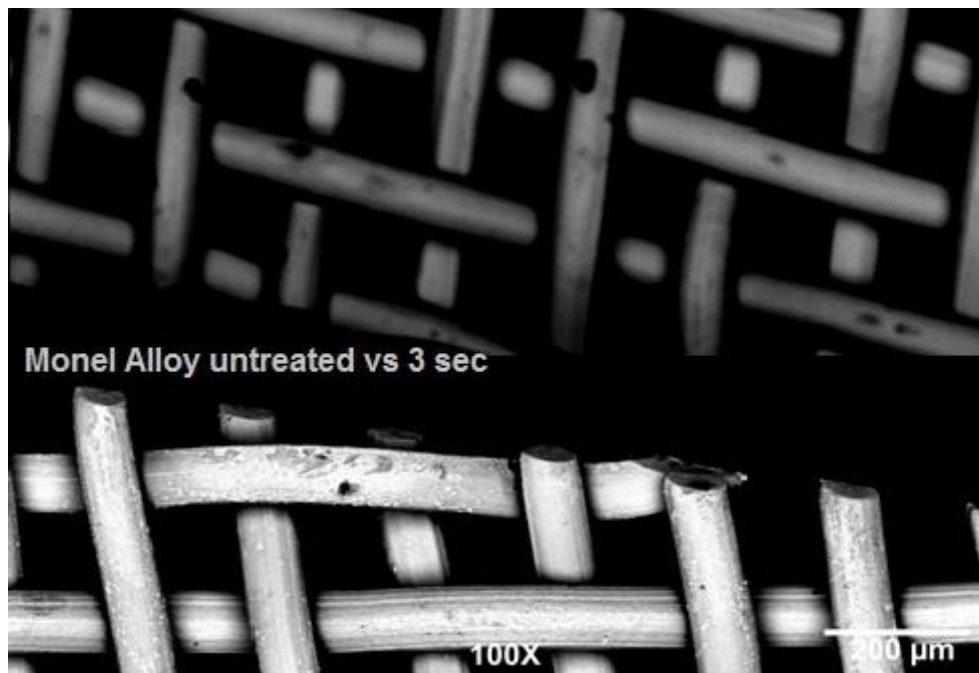


Figure 26. Top: 3 seconds activation; Bottom: Original Monel alloy mesh.

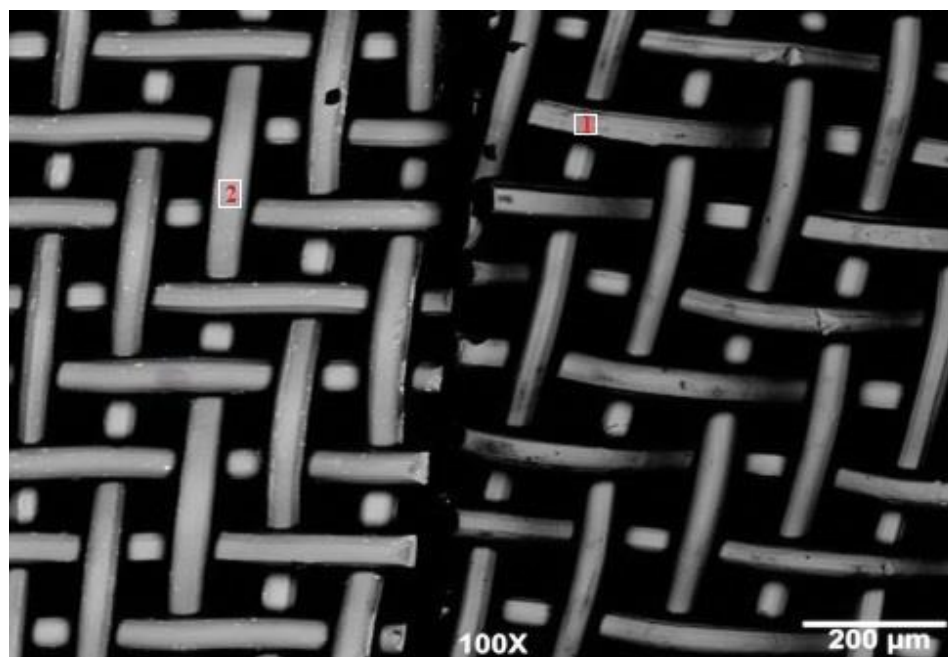


Figure 27. Monel gold-coated (left); Un-coated Monel alloy (right).

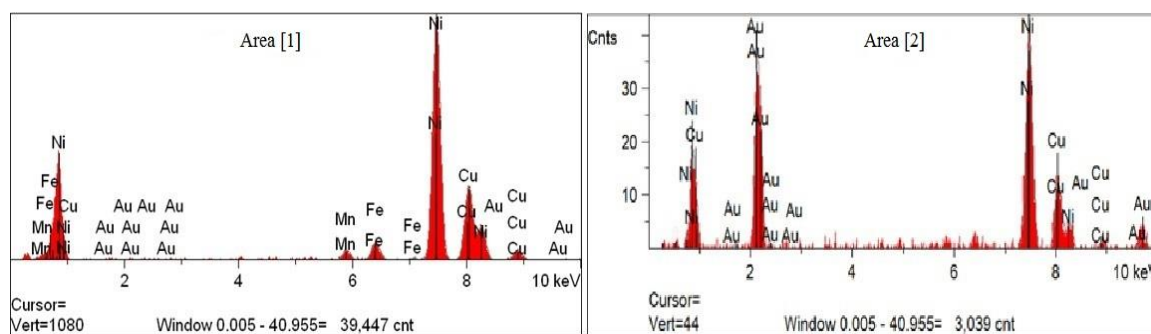


Figure 28. Elemental analysis of areas (1) and (2) in Figure 27.

3.5.1 Eventual failure of Monel column material following multiple electrochemical experiments.

The content of the highly corrosive activation solution that was necessary to prepare Monel alloy for gold deposition demonstrates its natural ability to withstand acidic and electrochemical attack. The resulting gold plated Monel was a column material capable of supporting electrochemical analysis within the redox potentials of gold. These potentials are dependent on concentration and composition of the electrolyte as well as the physical conditions of the chemical system. Testing potentials for electrochemical analysis were ± 1 V. These potentials were within referenced values of cited literature [31].

Assembled column material produced consistent electrochemical data for approximately 3-4 months. The daily number of the conducted tests were 3-4 tests on average. Change in column performance characteristics was abrupt and pronounced and was consistent with an acute failure in the column material. This material failure was an unanticipated setback and studies were conducted to determine the nature of the loss of the column function. SEM studies in Figure 29 revealed the extent of corrosion damage on the Monel column. Upon closer inspection, Figure 30 revealed excessive fracturing and peeling of the gold layer in addition to exposed Monel alloy showing evidence of substantial corrosion. Elemental analysis was performed on the very same SEM image of Figure 30. Integration data of the elemental analysis was commensurate to the area sampled within the numbered boxes. The red numbers correlate to their respective integrations found below (Figure 31). Integration data from area 1 corresponding to Figure 32, identified gold that was still intact and bonded with the Monel alloy. While,

area 2 represents the exposed area of the Monel alloy. The isolated nickel and copper peaks, suggest the common nickel and copper composition percentages indicative of Monel alloy. Whereas, area 3 and area 4 were elemental studies of the corrosion itself. Elemental analysis of these two areas revealed a high carbon and oxygen content in addition to nickel and copper. The high presence of carbon is substantial proof of polymerization of the primary surfactant (SDS) utilized in the electrochemical test carried out with the column. The high oxygen content found within the polymerizations is strong evidence suggesting ligand formation (hydrates). These coordination complexes are commonly found within the hydrated crystalline constructs of CuSO_4 and NiSO_4 . Both of these hydrated crystalline compounds are greenish blue in appearance. This was the color of the visible corrosion found on the column material after disassembly and before analysis with electron microscopy (Figure 33).

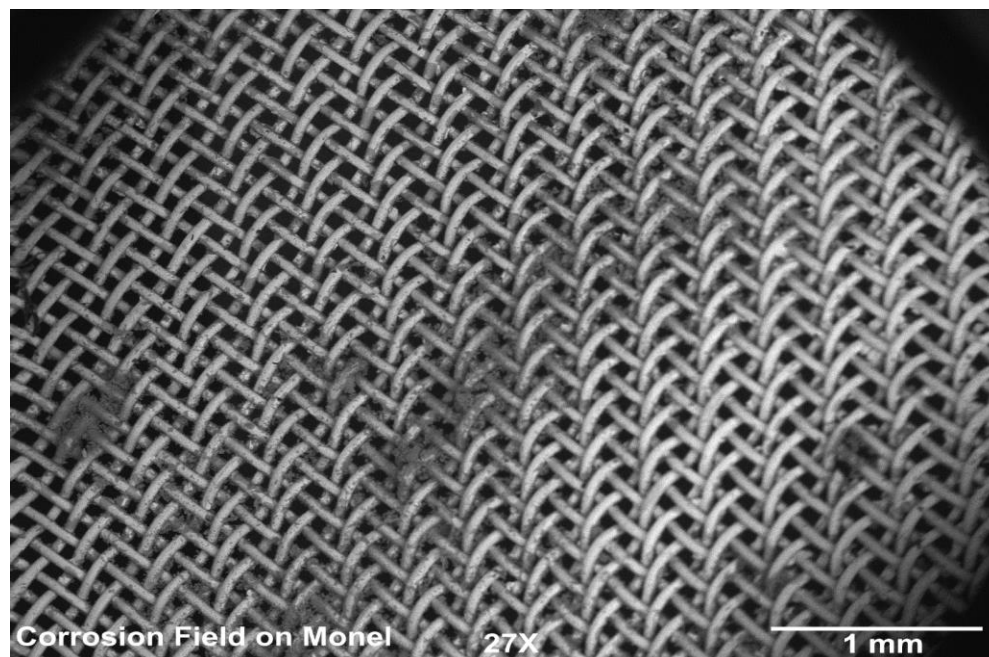


Figure 29. SEM image of the corrosion field of the Monel alloy.

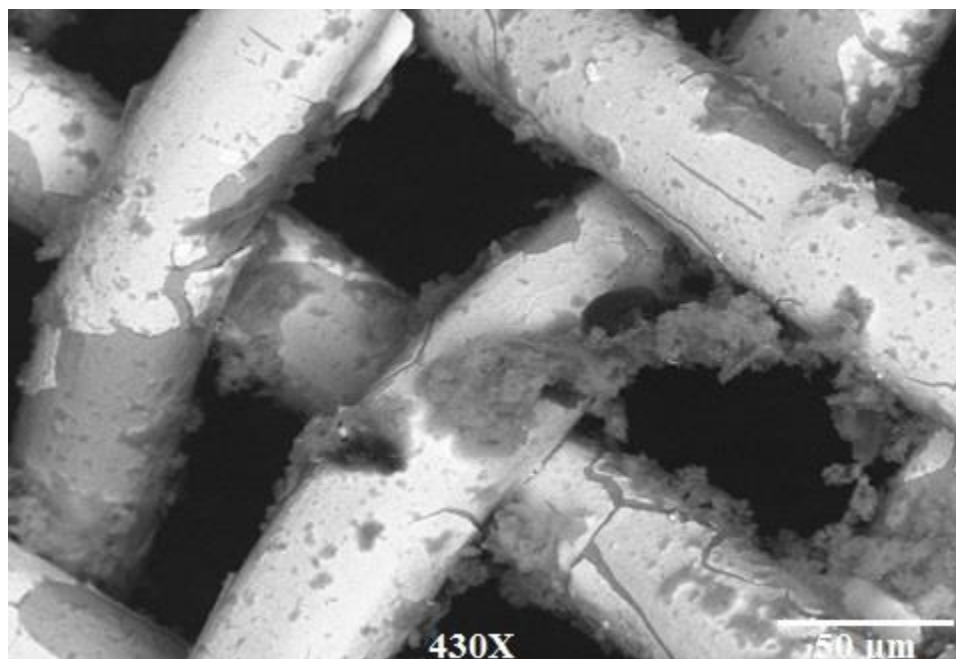


Figure 30. Plating fracture and exposed Monel alloy.

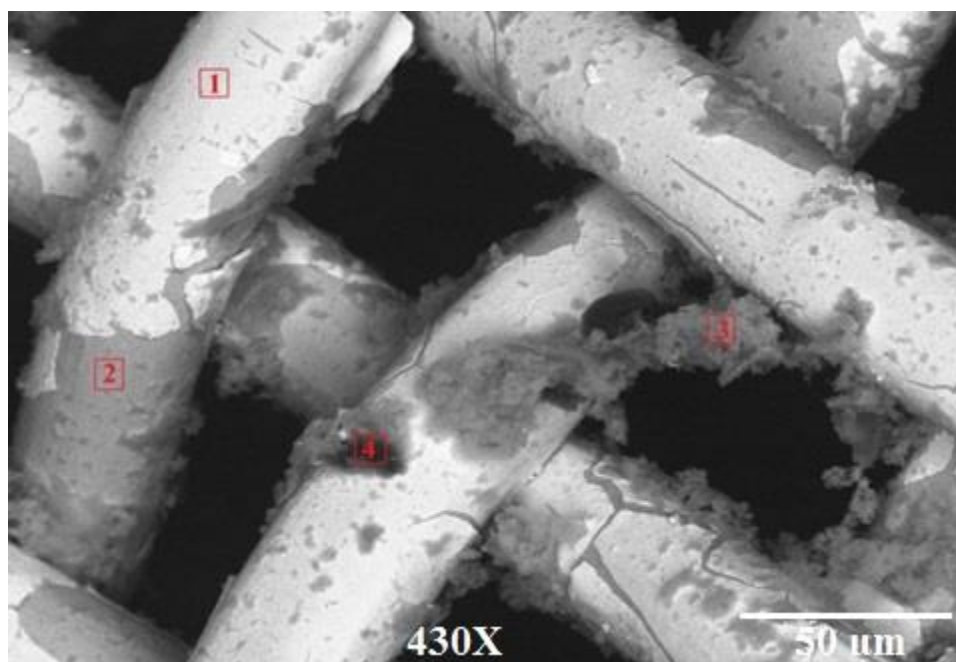


Figure 31. SEM image marked with integration data of the elemental analysis of Monel column material.

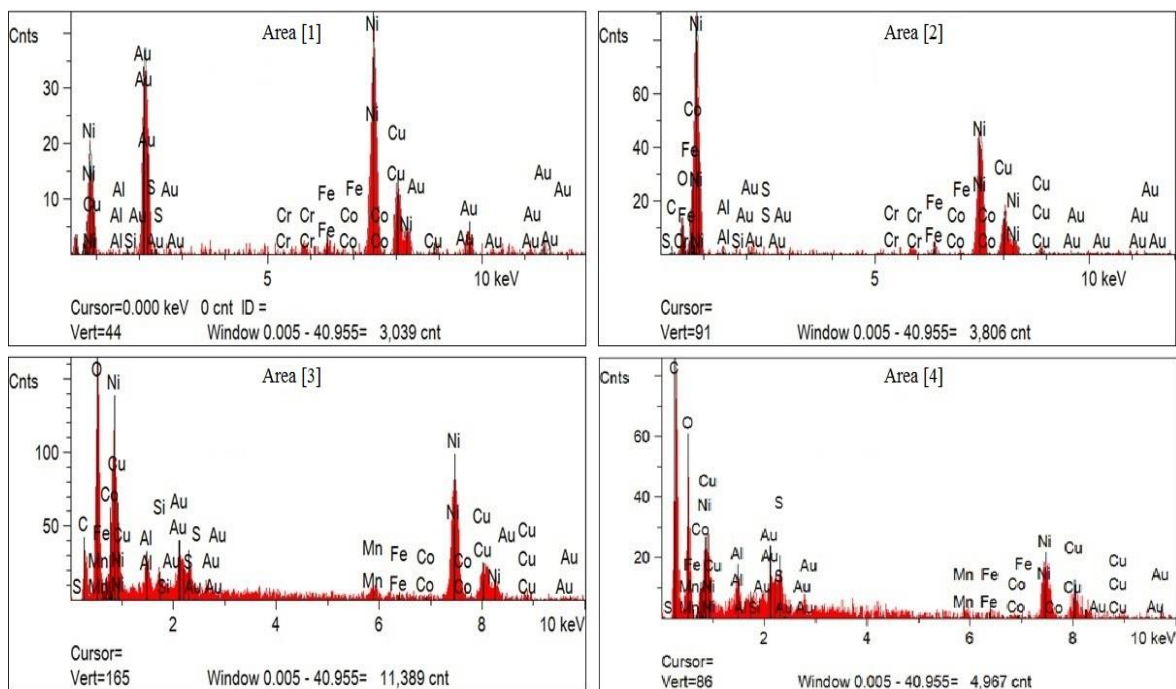


Figure 32. Elemental analysis of areas (1, 2, 3, and 4) in Figure 31.

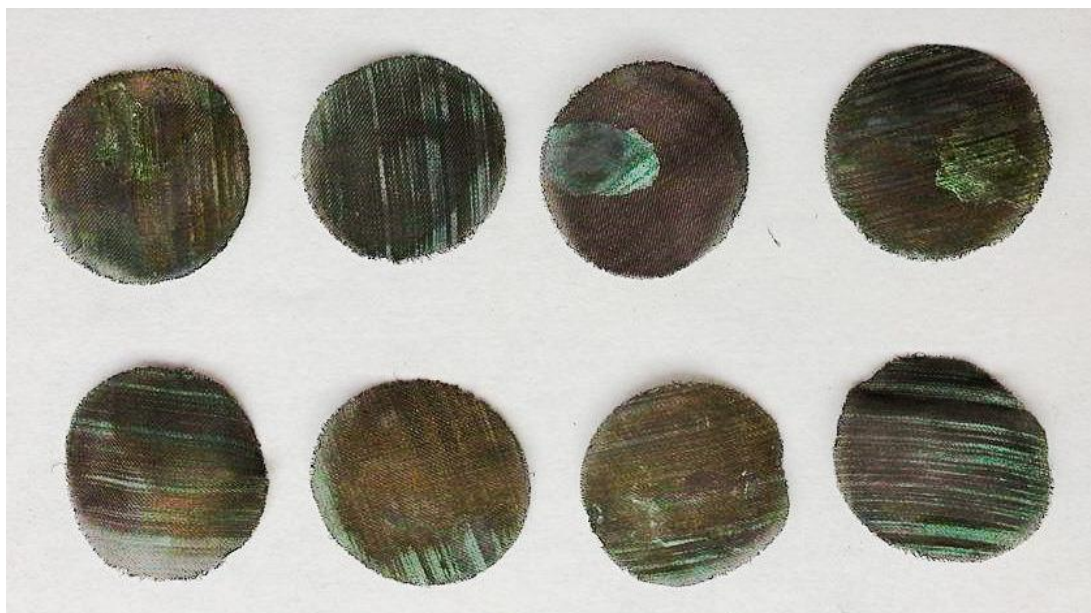


Figure 33. The visible corrosion of the column material after disassembly and before analysis with SEM.

3.6 The process of nickel coated with gold: scanning electron microscope SEM images

As shown in Figure 34, two distinctive areas were shown. The bright area represents the nickel gold-coated, and the brightness of this area was due to the gold layer on which was plated nickel. Whereas, the uncoated nickel mesh areas had less brightness than the gold-coated areas. However, another SEM image was taken for bare nickel mesh (Figure 35). In addition, the elemental analysis for the bare nickel was performed to see what other possible elements may exist in bare nickel mesh. It was observed that this nickel mesh consisted of about 99.8% nickel and less than 0.2% impurities that can be ignored (Figure 36), and no gold amount was observed.

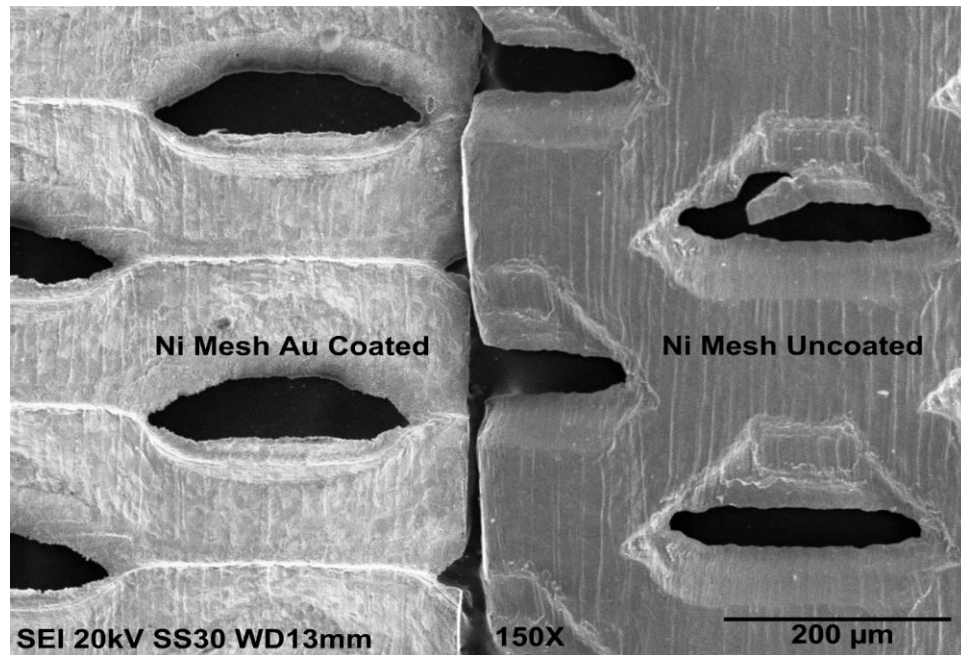


Figure 34. SEM image for nickel gold-coated and uncoated nickel mesh.

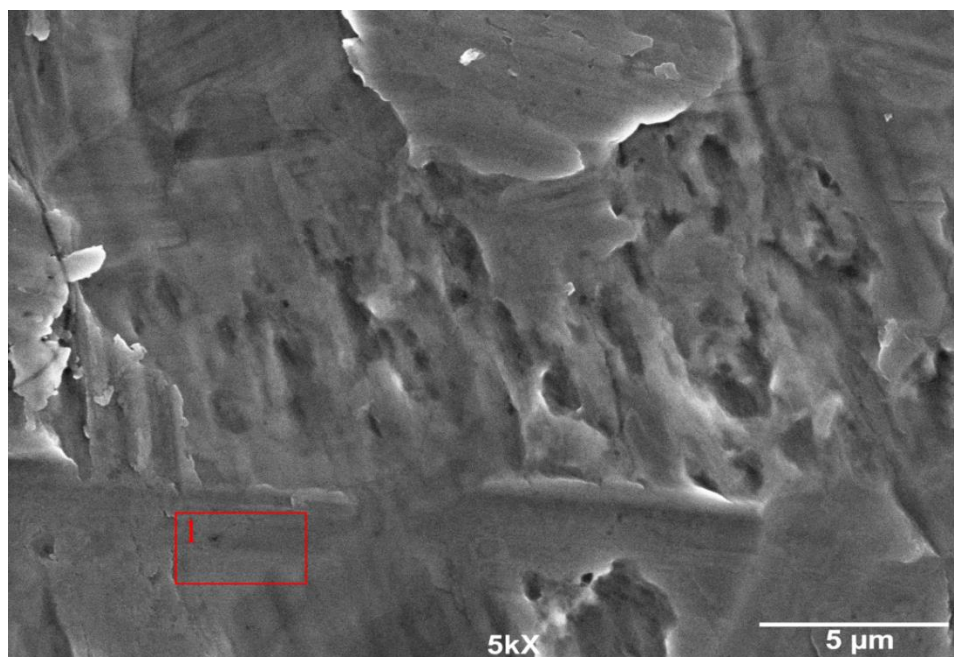


Figure 35. A magnified SEM image for the uncoated nickel mesh at 5kX using SEI mode.

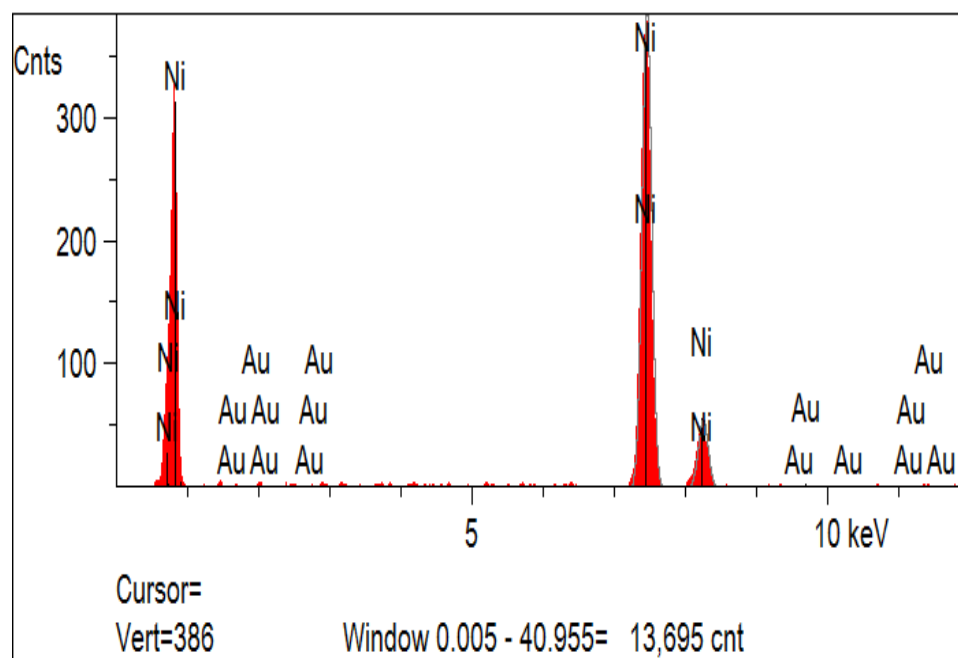


Figure 36. Elemental analysis of area (1) in Figure 35.

However, the first attempt to make sure that the plating procedure was successful, a quick wiping test was done using a tape. After the wiping test, it could be said that the coated gold was successfully plated on nickel and did not come off. Furthermore, SEM images were taken for further investigations. In addition, SEM images were taken using two different SEM modes: Secondary Electron Imaging mode (SEI) and Backscattered Electron Imaging (BEI) mode. However, in the SEI mode, the SEM images can be obtained with a highly topographical and high-resolution picture. In contrast, SEM images that obtained by BEI mode contain less topographical information. Additionally, the benefit of using BEI mode is to obtain more information about the elemental contrast, unambiguous observation of the gold coating (a uniform gold coating), and the capability of determining any possible defects in the gold coating. As shown in Figure 37, the SEM image was taken at 5kX magnification using SEI mode, the bright areas represent the condensed gold areas while the gray areas have less gold coating. Elemental analysis was performed for the two spots which are marked as area 1 and as area 2 in Figure 37. Figure 38, the elemental analysis for areas 1 and 2, higher gold abundance was observed for area 1 due to the existence of a gold layer on nickel in this area. In contrast, the elemental analysis for area 2 represents smaller nickel abundance peak. This was due to the existence of a condensed gold coating on the top of nickel. Likewise, another SEM image was taken at 5kX magnification using BEI mode for the topographical comparison and the investigation of possible defects in the gold coating (Figure 39). However, no defect was observed and the nickel plates were uniformly coated with gold. Finally, the last SEM image was taken at 20kX magnification using SEI mode for further topographical investigation (Figure 40). According to the obtained SEM's images, it could be concluded

that the gold was successfully plated onto nickel substrates to be used for analyte preconcentration procedure.

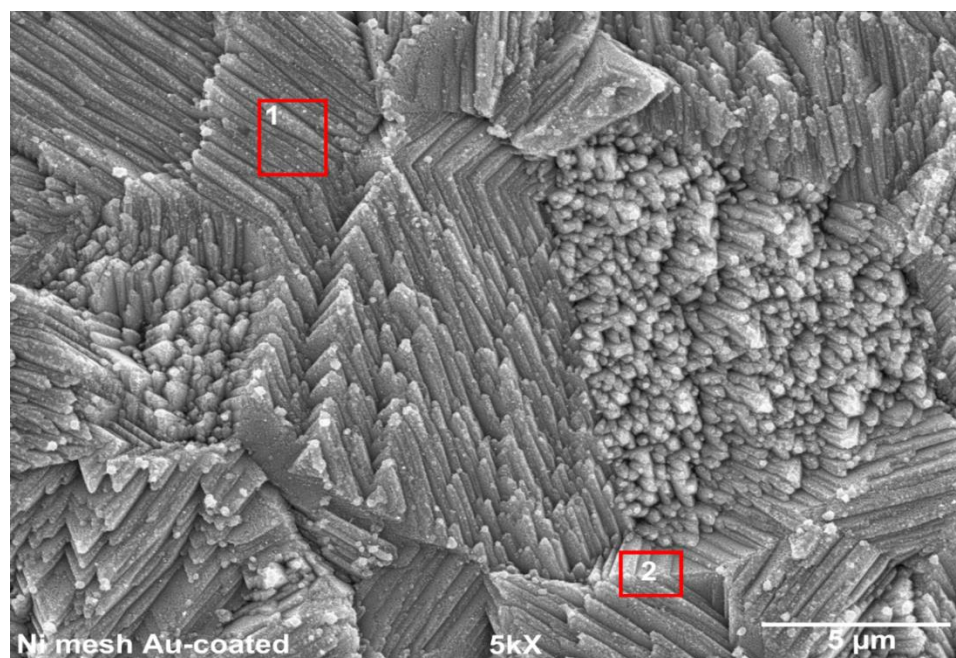


Figure 37. SEM image for nickel coated with gold at 10kX using SEI mode.

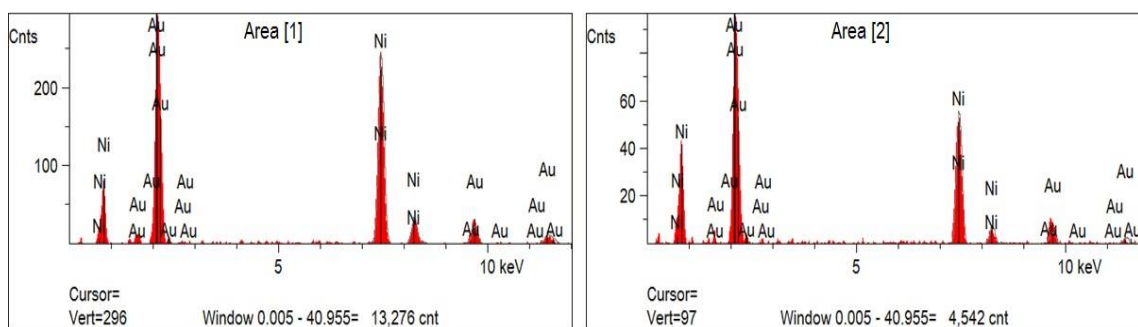


Figure 38. Elemental analysis of areas (1) and (2) in Figure 37.

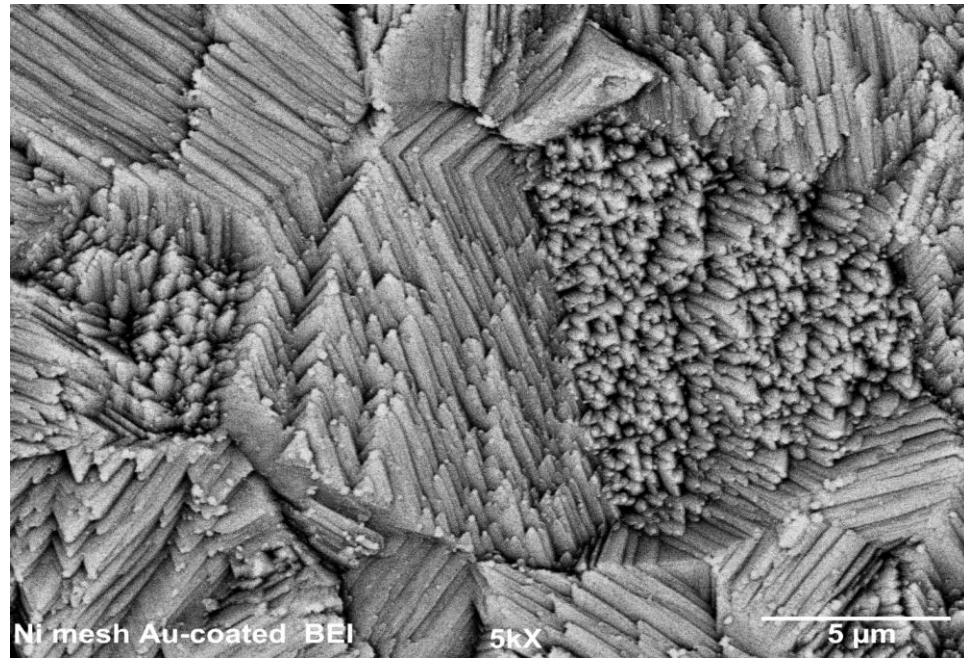


Figure 39. SEM image for nickel coated with gold at 5kX using BEI mode.

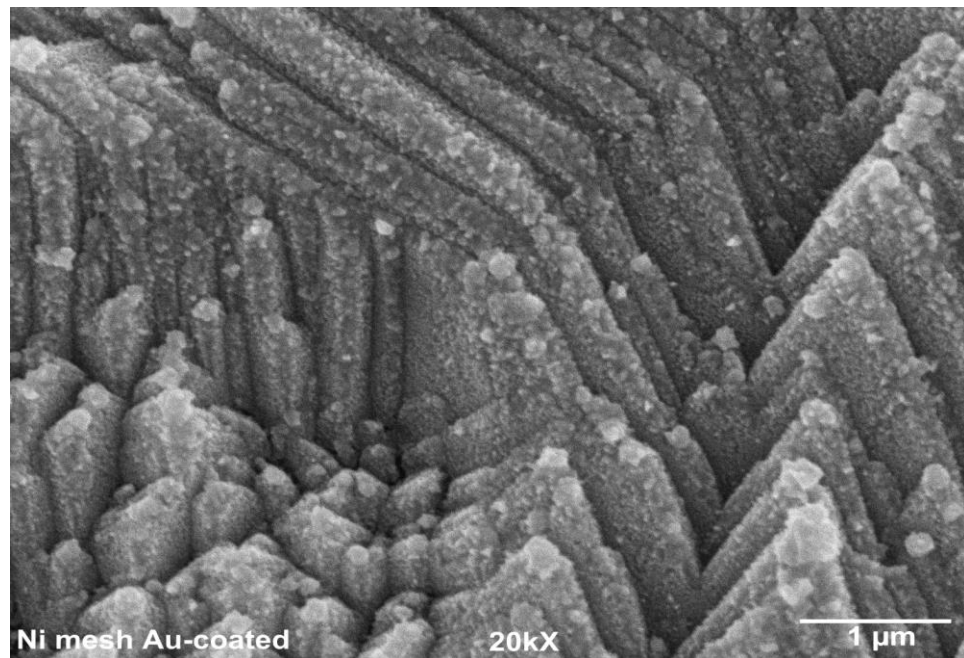


Figure 40. SEM image for nickel coated with gold at 20kX using SEI mode.

3.6.1 The evaluation of nickel gold-coated column

After more than 18 months of using nickel gold-coated column, SEM images were taken for the investigation of the robustness of gold coating. As shown in Figure 41, a SEM image was taken at 1kX using SEI mode. It was seen that there were two distinctive areas (marked in a red square). The area marked in Figure 41 was magnified 5kX for further investigation (Figure 42). The elemental analysis for the areas 1, 2, and 3 marked in Figure 42 was performed (Figure 43). As shown in Figure 43, the elemental analysis for area 1 revealed that there was no gold. This might be due to the friction which resulted from the rolling of the nickel gold-coated column when there was a need to take the column apart and clean it with methanol. Also, it might be due to the use for a long period. While, the analyses of area 2 and 3, confirm the existence of gold coating. The analyses of these areas represent smaller gold abundance peaks. This was also due to the use of the nickel gold-coated column for a long period which causing the gold coating layer to be attenuated and get thinner. Overall, according to SEM results, the performance of the nickel gold-coated column was effective even after 18 months of usage.

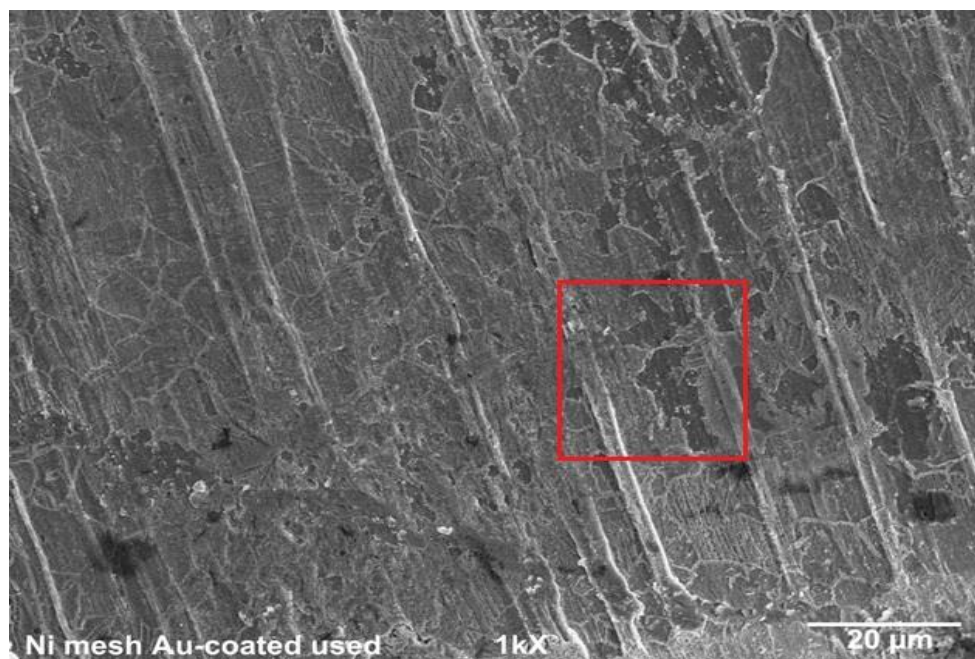


Figure 41. SEM image after 18 months for a used nickel gold-coated column at 1kX using SEI mode.

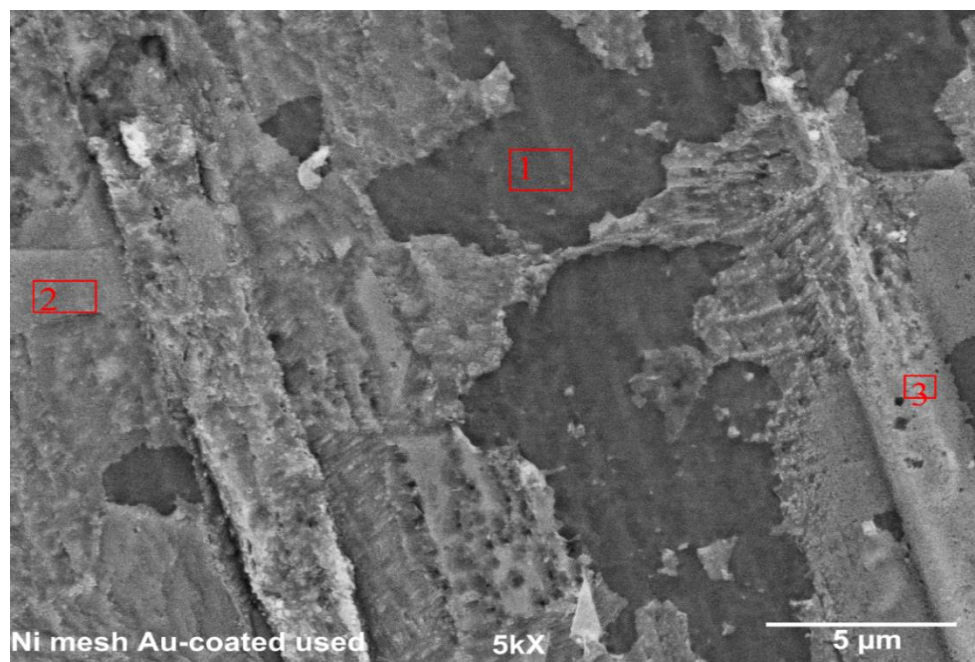


Figure 42. A magnified SEM image at 5kX for the area marked in Figure 41 using SEI mode.

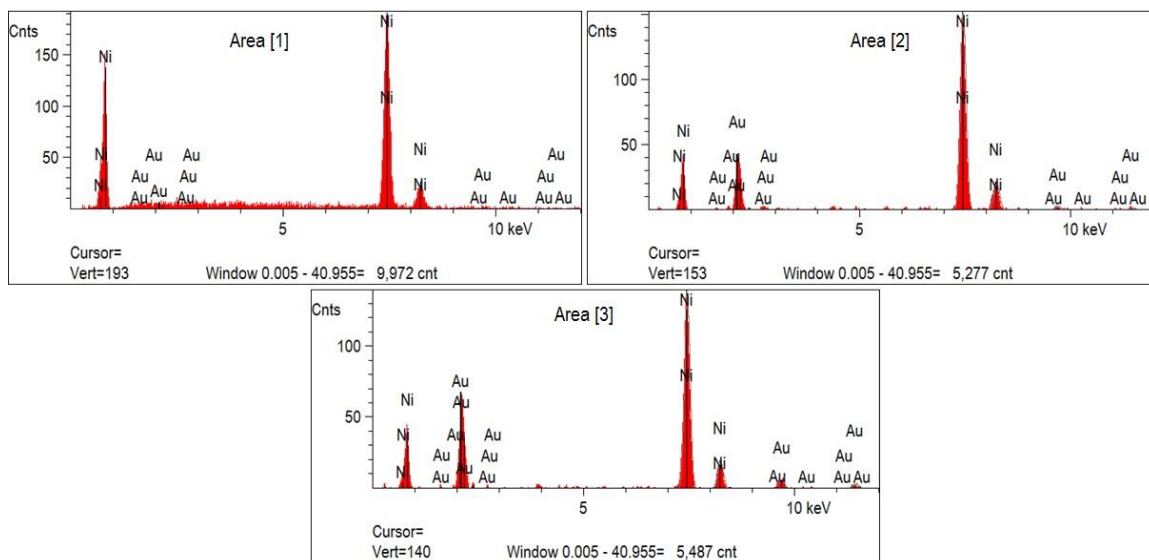


Figure 43. Elemental analysis of areas (1, 2, and 3) in Figure 42.

4. Conclusion

As a conclusion, micelles, admicelles, and hemimicelles are surfactant formations. It is important to note that solid-phase extraction is the most popular sample preparation method which is used for concentration, purification, and separation of the analyte. It is vital to note that the first stage of adsorption is determined by the nature of the head group. A significant point that the formation of DS surfactant monolayer (hemimicelle layer) on the positively charged gold substrates (planar gold) followed by the adsorption of 2-naphthol on this layer was monitored using capacitance measurements. Aiming for the high surface area, gold was coated on the various materials (woven Monel alloy and porous nickel). SEM was used for the investigation of gold plating. The nickel gold-coated column was exploited for the analyte preconcentration procedure. The preconcentration experiments were performed using various concentrations of SDS (4, 6, 16, and 32 mM) with 2 ppm 2-naphthol at an applied potential of 0.6 V vs. Ag/AgCl. Based on the HPLC results, a 20% drop in 2-naphthol concentration was observed at the extraction stage attributed to the adsorption of 2-naphthol onto DS surfactant monolayer. However, various control experiments were conducted in the absence of both an electric field and SDS to see whether there is a reduction in 2-naphthol concentration. In addition, electric field blank experiments were conducted at an applied potential of 0.6 V vs. Ag/AgCl. The used of an electric field at higher potentials resulted in a 20% drop in 2-naphthol concentration. Finally, anthracene and 9-anthracenecarboxylic acid were used as substituted test molecules instead of 2-naphthol. They both stuck too well to the gold substrates even with the absence of an electric field. As a conclusion, the electrical control of DS surfactants on gold surfaces for the analyte preconcentration prior

chromatographic analysis was not successful in preconcentrating the tested organic analytes.

5. Bibliography

1. Thurman, E.M.; Mills, M.S. Solid-Phase Extraction: Principles and Practice. *Wiley*; 1998.
2. Zaghbani, N.; Hafiane, A.; Dhahbi, M. Removal of Eriochrome Blue Black R from wastewater using micellar-enhanced ultrafiltration. *J Hazard Mater.* 2009, 168(2):1417-1421. doi: 10.1016/j.jhazmat.2009.03.044.
3. Noorashikin, MS.; Raoov, M.; Mohamad, S.; Abas, MR. Cloud point extraction of parabens using non-ionic surfactant with cyclodextrin functionalized ionic liquid as a modifier. *Int J Mol Sci.* 2013, 14(12):24531-24548. doi:10.3390/ijms141224531.
4. Bohidar, HB. COACERVATES: A NOVEL STATE OF SOFT MATTER — AN OVERVIEW. *J Surf Sci Technol.* 2008, 24(4):105-124.
5. Kamiński W, Kwapiński W. Applicability of Liquid Membranes in Environmental Protection. *Polish J Environ Stud.* 2000, 9(1):37-43.
6. Lun LEE K, Chieng CHONG C. The use of Reverse Micelles in Downstream Processing of Biotechnological Products. 2011.
7. Merino F, Rubio S, Pérez-Bendito D. Evaluation and optimization of an on-line admicelle-based extraction-liquid chromatography approach for the analysis of ionic organic compounds. *Anal Chem.* 2004, 76(14):3878–86.
8. Burgess, I.; Jeffery, C. A.; Cai, X.; Szymanski, G.; Galus, Z.; Lipkowski, J. Direct visualization of the potential-controlled transformation of hemimicellar aggregates of dodecyl sulfate into a condensed monolayer at Au(III) electrode surface, *Langmuir.* 1999, 15, 2607-2616.

9. Gangula, S.; S.-Y. Suen.; Conte, E. D. Analytical applications of admicelle and hemimicelle solid phase extraction of organic analytes, *Microchem. J.* 2010, 95, 2-4.
10. Gowardhane AP.; Kadam NV.; Dutta S. Review on Enhancement of Solubilization Process. *Am J Drug Discov Dev.* 2014, 4(2):134-152. doi:10.3923/ajdd.2014.134.152.
11. J.L. O'Haver.; J.H. Harwell. Adsolubilization, *ACS Symposium Series*, vol. 615, 1995, pp. 49–66, (Surfactant Adsorption and Surface Solubilization).
12. Forland G.M.; Rahman, T.; Høiland, H.; Borge, K.J. Adsorption of sodium dodecyl sulfate and butanol onto acidic and basic alumina, *Journal of Colloid and Interface Science.* 1996, 182 (2), 348 355.
13. Saitoh, T.; Matsushima, S.; Hiraide, M. Concentration of polyaromatic hydrocarbons in water to sodium dodecyl sulfate- γ -alumina admicelle, *Journal of Chromatography, A* 1069 (2) (2005) 271–274.
14. Saitoh, T.; Nakayama, Y.; Hiraide, M. Concentration of chlorophenols in water with sodium dodecylsulfate-alumina admicelles for high-performance liquid chromatographic analysis, *Journal of Chromatography, A* 972 (2) (2002) 205–209.
15. Saitoh, T.; Kondo, T.; Hiraide, M. Rapid and efficient admicelle-mediated extraction of chlorophenols in water, *Bulletin of the Chemical Society of Japan*, 79 (5) (2006) 748–750.
16. Saitoh, T.; Kondo, T.; Hiraide, M. Concentration of chlorophenols in water to dialkylated cationic surfactant-silica gel admicelles, *Journal of Chromatography, A* 1164 (1-2) (2007) 40–47.

17. Saitoh, T.; Matsushima, S.; Hiraide, M. Aerosol-OT- γ -alumina admicelles for the concentration of hydrophobic organic compounds in water, *Journal of Chromatography*, A 1040 (2) (2004) 185–191.
18. Lunar, L.; Rubio, S.; Perez-Bendito, D. Analysis of linear alkylbenzene sulfonate homologues in environmental water samples by mixed admicelle-based extraction and liquid chromatography/mass spectrometry, *Analyst*. 2006, 131(7), 835–841.
19. Wang, W.; Chen, B.; Huang, Y. Eggshell membrane-based biotemplating of mixed hemimicelle/admicelle as a solid-phase extraction adsorbent for carcinogenic polycyclic aromatic hydrocarbons, *Journal of agriculture and food Chemistry*. 2014, 62(32), 8051-8059.
20. García-Prieto A.; Lunar, L.; Rubio, S.; Pérez-Bendito, D. Hemimicelle-based solid-phase extraction of estrogens from environmental water samples, *Analyst*. 2006, 131:3, 407-414.
21. T.-Y. Wang.; G.-L. Chen.; C.-C. Hsu.; Vied, S.; Conte, E. D., S.-Y. Suen. Octadecyltrimethylammonium surfactant-immobilized cation exchange membranes for solid-phase extraction of phenolic compounds, *Microchem. J.* 96 (2010) 290–295.
22. T.-Y. Wang.; C.-H. Hsu.; T.-P. Chen.; Conte, E. D., Fenner, D.; Crossley, L.; Honeyman, C. H.; S.-Y. Suen. Adsorption of phenolic compounds onto trimethylstearylammmonium surfactant-immobilized cation-exchange membranes, *Microchemical Journal*. 99 (2011) 388–393.
23. Burgess, I.; Jeffrey, C.A.; Cai' X.; Szymanski, G.; Galus, Z.; Lipkowski, J. Direct visualization of the potential-controlled transformation of hemimicellar aggregates of

- dodecyl sulfate into a condensed monolayer at the Au (111) electrode surface. *Langmuir*. 1999,15(8):2607-2616. doi:10.1021/la981023i.
24. Chen, M.; Burgess, I.; Lipkowski, J.; Potential controlled surface aggregation of surfactants at electrode surfaces, *Surf Sci*. 2009, 603, 1878–1891.
 25. J.N. Israelachvili, D.J. Mitchell, B.W. Ninham, J. Chem. Soc. Faraday Trans. II 72 (1976) 1525.
 26. U. Retter, A. Avranas, *Langmuir*. 17 (2001) 5039.
 27. U. Retter, M. Tchachnikova, A. Avranas, J. *Colloid Interface Sci*. 251 (2002) 94.
 28. Burgess, I.; Zamlynny, I.; Szymanski, G.; Lipkowski, J.; Majewski, J.; Smith, G.; Satija, S.; Ivkov, R. Electrochemical and neutron reflectivity characterization of dodecyl sulfate adsorption and aggregation at the gold-water interface, *Langmuir*. 2001, 17, 3355-3367.
 29. Lee S. Electrically Controlled Formation and Release of Admicelles for Solid Phase Extraction. *Western Kentucky University Top SCHOLAR*. 2014, pp. 9-11.
 30. Skoog, DA.; Holler, FJ.; Crouch, SR. Principles of Instrumental Analysis. 6th ed. *Australia: Brooks/Cole; Thomson Learning; 2007*.
 31. Schlesinger, M.; Paunovic, M. Modern Electroplating. *Wiley; 2010*.